UCRL-10457 (corrected)

University of California

Ernest O. Lawrence
Radiation Laboratory

ANALYSIS OF ENHANCED DIFFUSIVITY IN NICKEL

Berkeley, California

DISCLAIMER

Research and Development

UCRL-10457
UC-25 Metals, Ceramics,
and Materials
TID-4500 (17th Ed.)

UNIVERSITY OF CALIFORNIA

Lawrence Radiation Laboratory
Berkeley, California

Contract No. W-7405-eng-48

ANALYSIS OF ENHANCED DIFFUSIVITY IN NICKEL

Ahmed Rassem Wazzan
(Ph.D. Thesis)

August 1962

Printed in USA. Price $1.75. Available from the
Office of Technical Services
U. S. Department of Commerce
Washington 25, D.C.

UCRL-10457

ANALYSIS OF ENHANCED DIFFUSIVITY IN NICKEL

Ahmed Rassem Wazzan

Lawrence Radiation Laboratory
University of California
Berkeley, California

August 1962

INTRODUCTION

The theory of diffusion in solids has been the subject of a great deal of investigation and satisfactory theoretical models have been constructed that adequately describe the basic diffusion processes in many simple solids.

The atomic process responsible for the observed effects of diffusion is generally accepted to be the random motion which each atom performs as a result of thermal agitation.[1] In particular, in a solid crystal, the mean time of stay of an atom at any one lattice site is assumed to be finite, the atom jumping from one site to the neighboring site and then to another, thus performing a random walk throughout the crystal. In substitutional solid solution, the jumps are most probably made via vacant lattice sites (vacancy diffusion) and a particular atom succeeds in making a jump only when a vacant site becomes adjacent to it as a result of the movement of the other atoms.

The features of such a random walk which are usually accessible to experiment are statistical quantities like $\overline{X}(t)$ the average net displacement and $\overline{X^2}(t)$ the average square of the net displacement X of an atom after a time t, measured along a given direction, the x-axis, the averages being taken over a very large number of identical particles. For example, there exists a simple relation between $\overline{X^2}(t)$ and the diffusion coefficient D, namely:[1]

$$D = \tfrac{1}{2}\, n \overline{\chi^2} \qquad (1)$$

where n = number of displacements suffered by the particle per unit time.

Eqn. (1) is valid for random walks which take place in chemically homogeneous systems (self-diffusion).

Next, we present Chandrasekhar's[1] method for obtaining Eqn. (1). Consider the simple one-dimensional random walk problem where a particle suffers displacements along a straight line in the form of a series of steps of equal length, χ, each step being taken in the forward or backward direction with equal probability, 1/2. After taking N such steps at the rate of N steps per unit time, the particle could be at any of the points:

$$-N, -N+1, \ldots, -1, 0, \ldots, N-1 \text{ and } N$$

The probability $W(\chi, t)\,\Delta\chi$ that the particle be found between χ and $\chi + \Delta\chi$ after a time, t, is given by

$$W(\chi,t)\,\Delta\chi = \frac{1}{2\left(\pi t n \frac{\overline{\chi^2}}{2}\right)} Exp\left[-\chi^2 \Big/ 4\left(t n \frac{\overline{\chi^2}}{2}\right)\right]\Delta\chi \qquad (2)$$

Chandrasekhar[1] reduces the problem of random walk for large N to a boundary value problem and obtains the following differential equation for $W(\chi,t)$:

$$\frac{\partial W}{\partial t} = \frac{n\overline{\chi^2}}{2}\,\frac{\partial W}{\partial \chi^2} \qquad (3)$$

And it can be shown by direct substitution that $W(x,t)$ as given by Eqn. (2) is the fundamental solution to this differential Eqn. (3). One also recognizes that Eqn. (3) is the standard form of the diffusion equation in one dimension

$$\frac{1}{D}\frac{\partial W}{\partial t} = \frac{\partial^2 W}{\partial x^2} \tag{4}$$

with D being equal to $1/2\, n\overline{x^2}$

Phenomenological definition of the diffusion coefficient D:

In the macroscopic theory of diffusion if $W(x,t)$ denotes the concentration of the diffusing atom at x and time t, then the amount crossing a unit area per unit time, the flux J, is given by

$$\vec{J} = -D\left(d\vec{n} \cdot \text{grad}\, W\right) \tag{5}$$

where $d\vec{n}$ = a unit vector in the direction of the flux.

The diffusion equation is a consequence of this relation and the continuity equation which also relates W to J in the following manner:

$$\frac{\partial W}{\partial t} = -\,\text{div}\,\vec{J} \tag{6}$$

Consequently, we may describe the motion of a large number of particles describing random walks without mutual interaction as a process of diffusion with the diffusion coefficient D being equal to

$$D = 1/2\, n\overline{x^2} \tag{7}$$

Self-diffusion (diffusion of radioactive atoms):

The following development through Eq. (18) inclusive is due to A. D. LeClaire, Colloque Sur la diffusion a l'etat Solide 1958.

Consider a crystal in which there exists along the x-direction a concentration gradient of radioactive atoms of one species but which is otherwise homogeneous chemically. We wish to know the net rate of transfer of atoms across some reference plane χ_0 arising from their random motion.

Consider an infinitesimal layer $d\chi_i$ at χ_i. At t = 0 each atom within this layer begins its random walk. Let $W(\chi, t)$ be the relative probability that in time t an atom will have migrated a distance X from χ_i. Since the medium is homogeneous chemically, migrations of +X and -X are equally probable. So that the average displacement after time t of a large number of atoms is zero.

$$\bar{X} = \int_{-\infty}^{+\infty} \chi\, W(\chi, t)\, d\chi = 0 \qquad (8)$$

Similarly, all odd moments of $W(\chi, t)$, X^3, X^5, --- etc. are zero.

However, the average squared displacement $\bar{X}^2$ is not zero and after time t all the radioactive tracer atoms originally within the layer $d\chi_i$ will be spread out and distributed in a Gaussian manner about χ_i, $\bar{X} = 0$, see Fig. 1. The area under curve I is $\int C(\chi_i)d\chi_i$ where $C(\chi)$ is the tracer concentration at x. And the area under curve II which represents the distribution at time t of atoms originally contained within the element of area $d\chi_j$ is $\int C(\chi_j)d\chi_j$. The half width of each of the two curves is $(\bar{X}^2)^{1/2}$.

The shaded area A_i represents the number of tracer atoms from χ_i which are on the right hand side of χ_0 after time t, and area

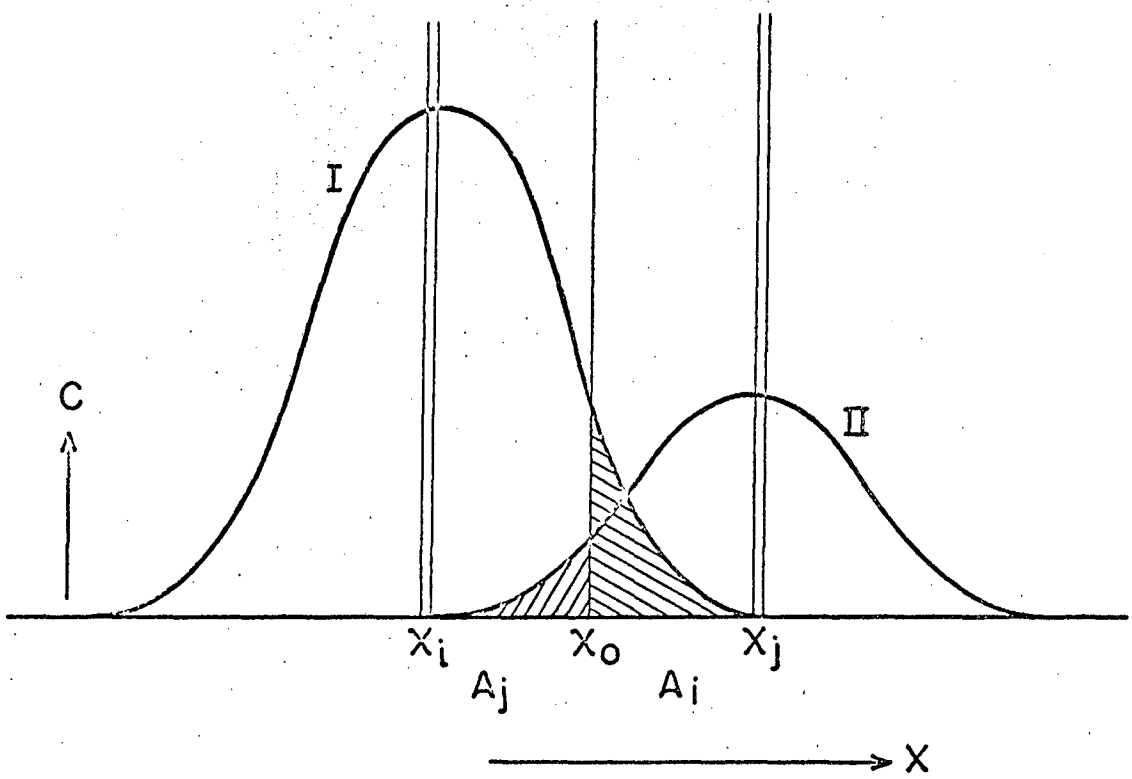

FIG. I THE GAUSSIAN DISTRIBUTION OF THE DIFFUSING ATOMS.

A_j the number from x_j now on the left hand side of x_o. Because area $A_i >$ area A_j, there has been a net flow of atoms across, and in the direction of decreasing concentration. The total net flow is obtained by summing the differences $A_i - A_j$ for all pairs of regions like dx_i and dx_j

The total number of tracer atoms originally on the left hand side of x_o which will be found on the right hand side after time t is,

$$\int_{-\infty}^{x_o} C(x) \left\{ \int_{x_o - x}^{\infty} W(x,t)\, dx \right\} dx \qquad (9)$$

the total integrand represents an area such as A_i. Similarly, the total number of atoms which have crossed x_o from right to left, i.e., the sum of areas like A_j, is:

$$\int_{x_o}^{+\infty} C(x) \left\{ \int_{-\infty}^{x_o - x} W(x,t) \right. \qquad (10)$$

The difference between Eqns. (9) and (10) gives the net transfer across x_o from left to right. If one expands $C(x)$ into a Taylor series about x_o:

$$C(x) = C(x_o) + \frac{\partial C}{\partial x}(x - x_o) + \tfrac{1}{2} \frac{\partial^2 C}{\partial x^2}(x - x_o)^2 + \cdots \qquad (11)$$

and substitute Eqn. (11) in Eqns. (9) and (10), then the difference between Eqns. (9) and (10) becomes

$$c(x_0)\left\{\int_{-\infty}^{x_0}\left(\int_{x_0-x}^{\infty} W(x,t)\,dx\right)dx-\int_{x_0}^{+\infty}\left(\int_{-\infty}^{x_0-x} W(x,t)\,dx\right)dx\right\}$$

$$+\frac{\partial c}{\partial x}\left\{\int_{-\infty}^{x_0}(x-x_0)\left(\int_{x_0-x}^{\infty} W(x,t)\,dx\right)dx-\int_{x_0}^{+\infty}(x-x_0)\left(\int_{-\infty}^{x_0-x} W(x,t)\,dx\right)dx\right\} \qquad (12)$$

$$+\tfrac{1}{2}\frac{\partial^2 c}{\partial x^2}\left\{\int_{-\infty}^{x_0}(x-x_0)^2\left(\int_{x_0-x}^{\infty} W(x,t)\,dx\right)dx-\int_{x_0}^{+\infty}(x-x_0)^2\left(\int_{-\infty}^{x_0-x} W(x,t)\,dx\right)dx\right\}$$

Integrating by part twice and dividing by t one obtains the average net rate of flow, the flux, J, :

$$\vec{J}=\frac{1}{t}\left\{c(x_0)\overline{X}-\frac{\partial c}{\partial x}\left(\frac{\overline{X^2}}{2!}\right)+\frac{\partial^2 c}{\partial x^2}\left(\frac{\overline{X^3}}{3!}\right)+\cdots\right\} \qquad (13)$$

But since for self-diffusion $\overline{X}$, $\overline{X^3}$, $\overline{X^5}$, etc., are zero, this becomes Fick's law:

$$\vec{J}=-\frac{\overline{X^2}}{2t}\frac{\partial c}{\partial x} \qquad (14)$$

Eqns. (14) and (6) will lead to the diffusion Eqn. (4) and hence

$$D_{s.d.}=\tfrac{1}{2}t\,\overline{X^2} \qquad (15)$$

If Γ is the average jump frequency of an atom, the total number of jumps after time t is $N=\Gamma t$. Let x_j denote the x component of the jth jump of an atom then:

$$\overline{X^2} = \overline{\left(\sum_{j=1}^{N} x_j\right)^2} = \overline{\sum_{j=1}^{N} x_j^2} + \sum_{j \neq j'} \overline{x_j x_{j'}} \qquad (16)$$

Since the averages are taken over a large number of atom paths the last term will be zero (positive and negative products will occur with equal frequency). Suppose now that when an atom makes a jump it has a choice of s directions (s = 12 for face-centered cubic metals) and let Γ_i be the jump frequency in the ith direction so that $\Gamma = \sum_{i=1}^{s} \Gamma_i$, and let x_i be the x component of the corresponding jump vector, then:

$$\begin{aligned} \overline{X^2}(t) = \overline{\sum_{j=1}^{N} x_j^2} &= N \overline{x_j^2} \\ &= (N/\Gamma) \sum_{i=1}^{s} \Gamma_i x_i^2 \\ &= t \sum_i \Gamma_i x_i^2 \end{aligned} \qquad (17)$$

Substituting for $\overline{X^2}$ into Eqn. (15) D becomes equal to

$$D = \tfrac{1}{2} \sum_{i=1}^{s} \Gamma_i x_i^2 \qquad (18)$$

For self-diffusion via the vacancy mechanism as is the case for nickel, the jump frequency of an atom Γ will be given by the number of times it tries to jump ν_0 ($\nu_0 \sim$ the Debye frequency) times the probability of finding a vacant lattice site P_v next to it times the probability of success in overcoming the energy barrier of the jump P_j or

$$\Gamma = \nu_0 P_v P_j \qquad (19)$$

where P_v = the concentration of vacancies $\frac{n_v}{n_s}$; where

n_v = number of vacancies per unit volume and

n_s = number of sites per unit volume and P_j ,

has the form P_j = constant $\times \exp(-\Delta G_m/kT)$ where

ΔG_m = free energy of motion of a vacancy.

If we assume that the Γ_i are all equal for self-diffusion in cubic crystals, the expression for the diffusion coefficient becomes:

$$D = 1/2 \nu_0 P_j \frac{n_v}{n_s} \sum_{i=1}^{s} \lambda_i^2 \qquad (20)$$

Because of the important role played by diffusion processes in many solid-state phenomena such as oxidation, the annealing of radiation damage, creep, and rupture, and in view of the wide variety of application in which materials are under strain, a thorough understanding of the effects of strain and strain rate on diffusion is highly desirable.

It is the purpose of this paper to investigate the effect of strain and strain rate on the coefficient of self-diffusion in single and polycrystalline nickel.

A direct observation of Eqn. (20) is that the diffusion coefficient is linearly dependent on the number of vacancies n_v . Hence, any possible mechanism for the formation of excess vacancies (over the thermal equilibrium number) will lead to the enhancement of D.

The effect of plastic straining on self-diffusion:

Excess vacancies can be generated by the thermally activated motion of jogged screw dislocations, the climb of edge dislocations and other perhaps less effective mechanisms such as the superposition of positive and negative edge dislocations on adjacent planes. Vacancies can

be annihilated by adsorption on the grain boundaries, adsorption in the form of atmospheres about dislocations, combination with solute atoms, direct combination with climbing edge dislocations or additions to screw dislocations, plus condensation by heterogeneous or homogeneous nucleation of voids.

When the generation of vacancies is stimulated by externally induced effects such as plastic straining, the number of vacancies present might temporarily exceed the equilibrium value for the annealed state. If the enhancement in the diffusion coefficient upon plastic straining is solely due to the increase in the number of vacancies and since substitutional diffusion is known to occur principally as a result of exchanges between vacancies and atoms, it is anticipated that excess vacancies arising from external effects might be "counted" by evaluating the number of vacancies that account for the observed enhancement in the diffusion coefficient.

Self-diffusion may also be enhanced during plastic straining by short circuiting along additional dislocations or sub-boundaries that are introduced in the structure upon plastic deformation.

The first major question to be answered concerns whether or not the excess vacancies, produced under plastic straining, are sufficiently numerous to provide a measurable increase in the diffusivity. As shown in Table I some preliminary results have already been reported by several authors which, in general, suggest that diffusion is enhanced during plastic straining. On the other hand the serious discrepancy between the data obtained by other investigators and those of Darby, Tomizuka and Balluffi require further study and elucidation.

The second question to be answered concerns whether or not short circuiting can account for the observed increase in the diffusion coefficient. Since the existing data, given in Table I, suggests that the most pronounced

Table I

Effects of Plastic Straining on the Coefficient of Self-diffusion

Ref. No.	Deformed Materials	Diffusing Elements	Type of Deformation	Method of Measurement	Strain rate/hr	Ds/Du
2	Coarse grained iron	Fe-55	Compression without lubrication at faces	Diffusion absorption	0 to 0.36	up to 16
3	"	"	Compression with lubrication at faces	"	"	up to 20
4	Ni	Hydrogen	Extension	--	"	1.0
5	Ag	Ag-110	Compression	Autoradiography	.00288	10
6	Single crystal Ag	"	"	Sectioning technique	0 to 0.36	1
7	Cu bicrystals	"	Shear parallel to grain boundary	"	0.3	1
8	Single crystal Ag	"	Torsion	"	0 to 0.72	up to 100
9	Fine grained Ag	Fe-59	Extension	Diffusion Absorption	0 to .0036	1
9	Fine grained Fe	Ag-110	Compression	"	0 to .36	1
10a, b	Cu-coarse grained	"	"	Diffusion absorption and sectioning technique	0 to 36	up to 20
					0 to 108	up to 20
11a, b	Low carbon steel, Ni, etc.	Fe-59	Extension	Sectioning technique	0 to .0036	up to 10
12	Ni-Mo alloys	Co-60 or Fe-59	Compression	Diffusion absorption	0 to .00036	up to 10

effects are obtained for high strain rates and low temperatures, an attempt was made to select the experimental procedures so as to obtain a most sensitive measure of the diffusivity. Toward this end it was decided to use surface counting techniques to ascertain the self-diffusion of Ni(63) as electroplated on the surface, into high purity nickel. Ni(63) is a low energy, about 60,000 volt, β , emitter having a half life of about 85 years. Since these β rays are highly absorbed, the diffusivity can be accurately measured by surface monitoring without taking recourse to the less accurate sectioning technique. Since polycrystalline nickel, as do other metals, exhibits intergranular fracturing during high temperature straining, it was considered necessary to employ single crystals for the purpose of studying the effect of creep rate on the diffusion coefficient, in order to avoid dangers of enhanced diffusion resulting from surface migration along fissures. On the other hand, single and polycrystals were used when studying the effect of cold work (strain) on the diffusion coefficient.

The results to be reported here reveal that the diffusivity is indeed enhanced as a result of plastic straining. A preliminary discussion and some tentative conclusions on possible mechanisms for the formation of vacancies are included in this paper.

EQUIPMENT AND PREPARATION OF SPECIMENS

Single crystals:

Nickel single crystals (0.020% C, 0.001% S, with only traces of Co and other impurities) were prepared using the Bridgman technique. Nickel was placed in high purity alundum boat contained in a mullite tube and heated by a water-cooled moving coil induction furnace. The nickel was heated under a high vacuum to the melting point and a favorable thermal

gradient was established by moving the induction coil along the axis of the mullite tube at the rate of three inches per hour. Each crystal was machined into rectangular shaped specimens of 4 x 0.5 x 0.1 inches, polished mechanically, then electrolytically to remove any possible effects of machining. After polishing, the specimens were plated with radioactive Ni (isotope Ni (63). The plated layer of Ni was estimated to be about 1000 atoms thick.

Polycrystals, rectangular shaped:

Polycrystalline nickel specimens (4 x 0.5 x 0.1 inches were annealed at 1100°C for several hours for homogenization then slowly cooled to room temperature. The final average grain diameter was about 0.1 mm. The specimens were then polished and deformed in tension (using the Instron) to various values of strains. The specimens were then polished electrolytically and plated with radioactive Ni using the same technique as that for the single crystals.

EXPERIMENTAL PROCEDURE

The effect of strain on self-diffusion:

a. Nickel polycrystalline specimens deformed at room temperature for strains ranging from 0.31 to 0.04 were plated with radioactive nickel, then given a series of diffusion anneals over the temperature range 675°C to 750°C.

b. Nickel single crystals plated with radioactive nickel were deformed over the temperature range 675°C to 750°C, to strains ranging from 0.33 to 0.06 then given a series of diffusion anneals over the temperature range 675°C to 750°C.

The effect of strain rate on self-diffusion:

Nickel single crystals plated with radioactive nickel were given a series of diffusion anneals followed by dynamic diffusion anneals where the specimens were annealed and strained simultaneously.

These anneals were carried out in a system consisting of a furnace with a ten-inch long U shaped tungsten heating element mounted inside a vacuum chamber. Two three-inch long cylindrical nichrome heating elements were placed at each end of the main coil to compensate for end heat losses. Each of the three elements was controlled separately and connected to a constant voltage source. The temperature of the furnace was measured by means of four chromel-alumel thermocouples placed 1/2 inch apart along the mid-section of the furnace. The specimen was held by self-tightening grips. Two calibrated chromel-alumel thermocouples placed 1/2 inch apart along the mid-section of the specimen were used to measure its temperature. The tensile machine head moved at a constant rate, thus providing almost a constant strain rate. The system was purged several times with argon, and finally the test was carried out in an atmosphere of argon.

The surface activity before and following each diffusion anneal was measured using a windowless flow counter employing Geiger gas (99% He plus 1% isobutane). The output of the counter was recorded on a Tracerlab Super-scalar. The surface radioactivity was measured at three positions in the center of the specimen after each anneal. The areas monitored were 1/4 inch diameter circles with 3/8 inch between centers. Ten samplings of 100,000 counts each were made to determine the activity at each position the counting rates being standardized and corrected in each instance for the "dead time" and the "back-ground count". Throughout the diffusion anneals fluctuations in the temperature of the specimen were less than + 1.5 C.

METHOD OF ANALYSIS

The effect of strain on self-diffusion:

A series of static diffusion anneals were carried out on deformed single and polycrystalline nickel specimens. Following each anneal, the

furnace was cooled rapidly at about 50°C per minute, and the specimen was withdrawn for a surface count. Upon the second anneal the specimen was heated rapidly at about 50°C per minute to the diffusion anneal temperature. The diffusivity at the end of each diffusion anneal was determined using the following relationship:[13]

$$I/I_o = e^{\rho} \operatorname{erf} \rho^{1/2} \tag{21}$$

where

$$\rho = \left(\mu e^{\epsilon_{xx}}\right)^2 \left(D_u t_u + \int_o^{t_s} D\, dt_s\right) \tag{22}$$

and I_o = initial surface activity at t = o,

I = surface activity at t = tu + ts,

D_u = static diffusion coefficient,

D_s = diffusion coefficient under conditions of plastic straining,

t_u = time of static anneal,

t_s = time of subsequent dynamic anneal,

μ = linear adsorption coefficient, and

ϵ_{xx} = true strain in the thickness direction,

$\overline{D}_s = \lim_{t_s \to \infty} \dfrac{\int_o^{t_s} D\, dt_s}{t_s}$

= the steady state diffusion coefficient under conditions of plastic straining.

The linear adsorption coefficient μ was determined from the change in surface activity with thickness of the radioactive isotope layer according to[14]

$$I_{s_1}/I_{s_2} = \frac{1 - e^{-\mu x_1}}{1 - e^{-\mu x_2}} \qquad (23)$$

where I_{s_i} = the measured surface intensity per unit area for plating thickness, and

x_i = radioactive isotope layer thickness.

As given by the data in Table II a mean value of $\mu_{av.} = 1.3 \pm 0.1 \times 10^{-4}$ cm^{-1} was obtained and the strain in the thickness direction was measured directly after each dynamic diffusion anneal.

For the case of static diffusion anneals $t_s = 0$ and $\epsilon_{xx} = 0$ Eqn. (22) reduces to

$$\rho = \mu^2 t_u D_u \qquad (24)$$

Eqn. (24) shows that ρ increases linearly with t_u, hence a plot of ρ vs. t_u will yield a straight line with a slope equal to $\mu^2 D_u$. The experimental values of I/I_0 were introduced into Eqn. (21) and the corresponding values of ρ were calculated. Plots of ρ vs. t were prepared as shown in Figs. 2,3,4,5,&6. A straight line was drawn through each set of points and its slope used to obtain a value for D_u. Table III lists the experimental and calculated results.

The effect of strain rate on self-diffusion:

A cyclic series of static and dynamic diffusion anneals were carried out on a number of nickel single crystals for various temperatures and strain rates. The surface activity following each anneal was determined. The coefficient D_u corresponding to the static anneals was determined as was

Table II

Determination of Absorption Coefficient μ

Specimen	1	2	3
Counts/sec-cm^2	1389	1663	1950
Thickness of Ni(63) cm	46.9×10^{-6}	61.2×10^{-6}	78.9×10^{-6}
I_1/I_2	.836	$\Rightarrow$	$\mu = 1.39 \times 10^4$ cm^{-1}
I_2/I_3	.848	$\Rightarrow$	$\mu = 1.21 \times 10^4$ cm^{-1}
I_1/I_3	.709	$\Rightarrow$	$\mu = 1.27 \times 10^4$ cm^{-1}
		Average	$\mu = 1.29 \times 10^4$ cm^{-1}

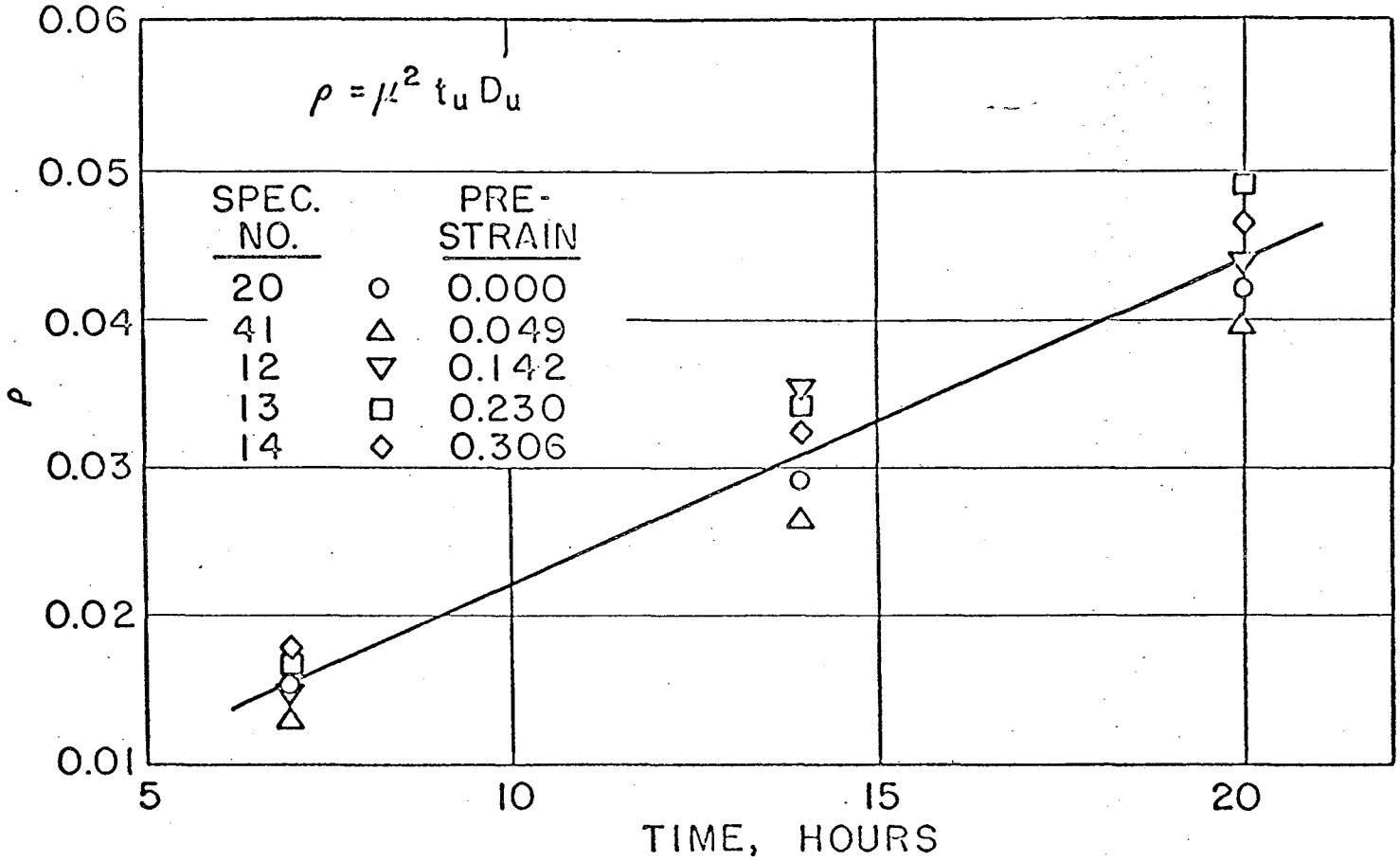

FIG. 2 ρ AS A FUNCTION OF TIME FOR STATIC DIFFUSION ANNEALS OF POLYCRYSTALLINE NICKEL SPECIMENS AT 948 ± 1.5°K.

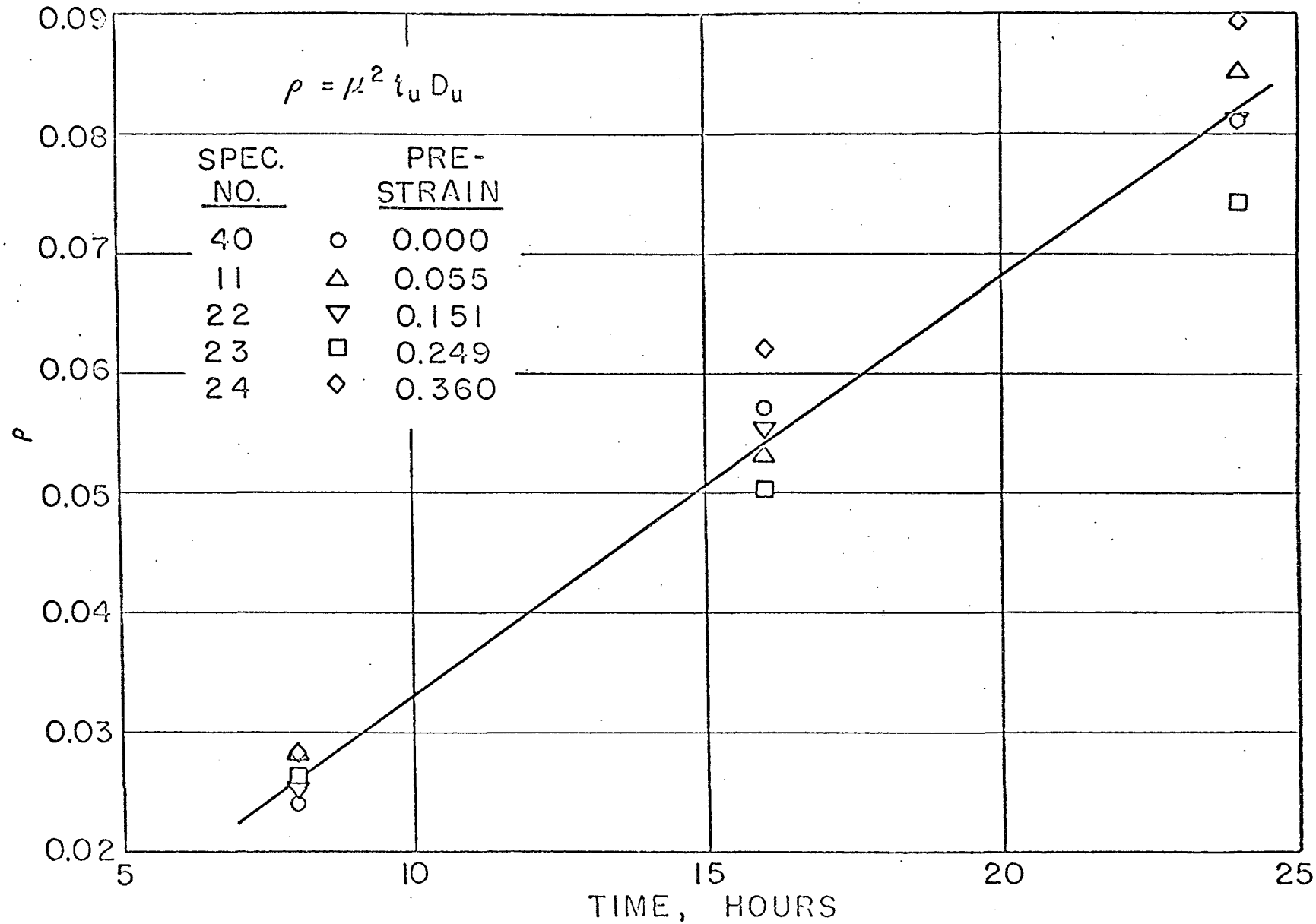

FIG. 3 ρ AS A FUNCTION OF TIME FOR STATIC DIFFUSION ANNEALS OF POLYCRYSTALLINE NICKEL SPECIMENS AT 973 ± 1.5 °K.

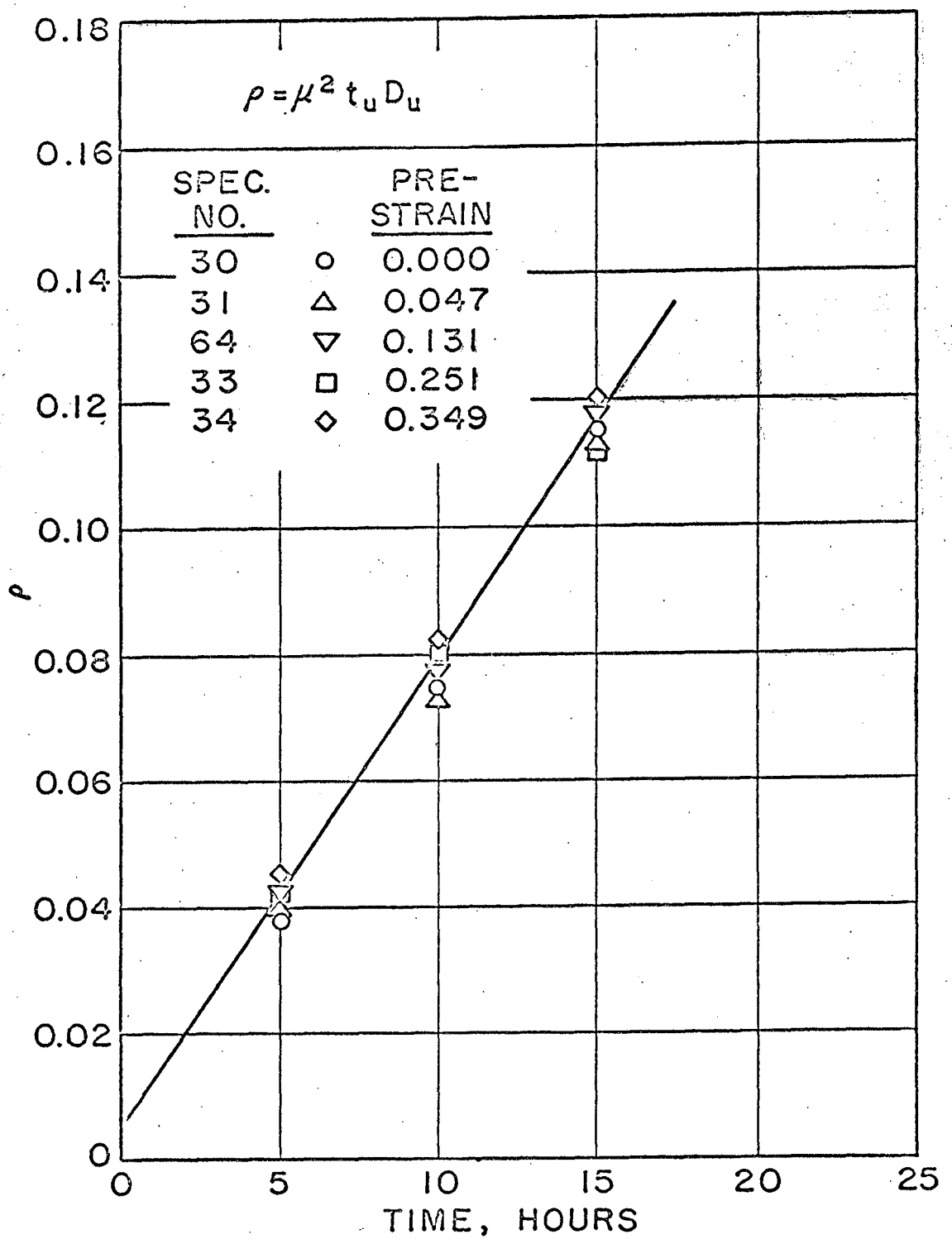

FIG. 4 ρ AS A FUNCTION OF TIME FOR STATIC DIFFUSION ANNEALS OF POLYCRYSTALLINE NICKEL SPECIMENS AT 1023 ± 1.5 °K.

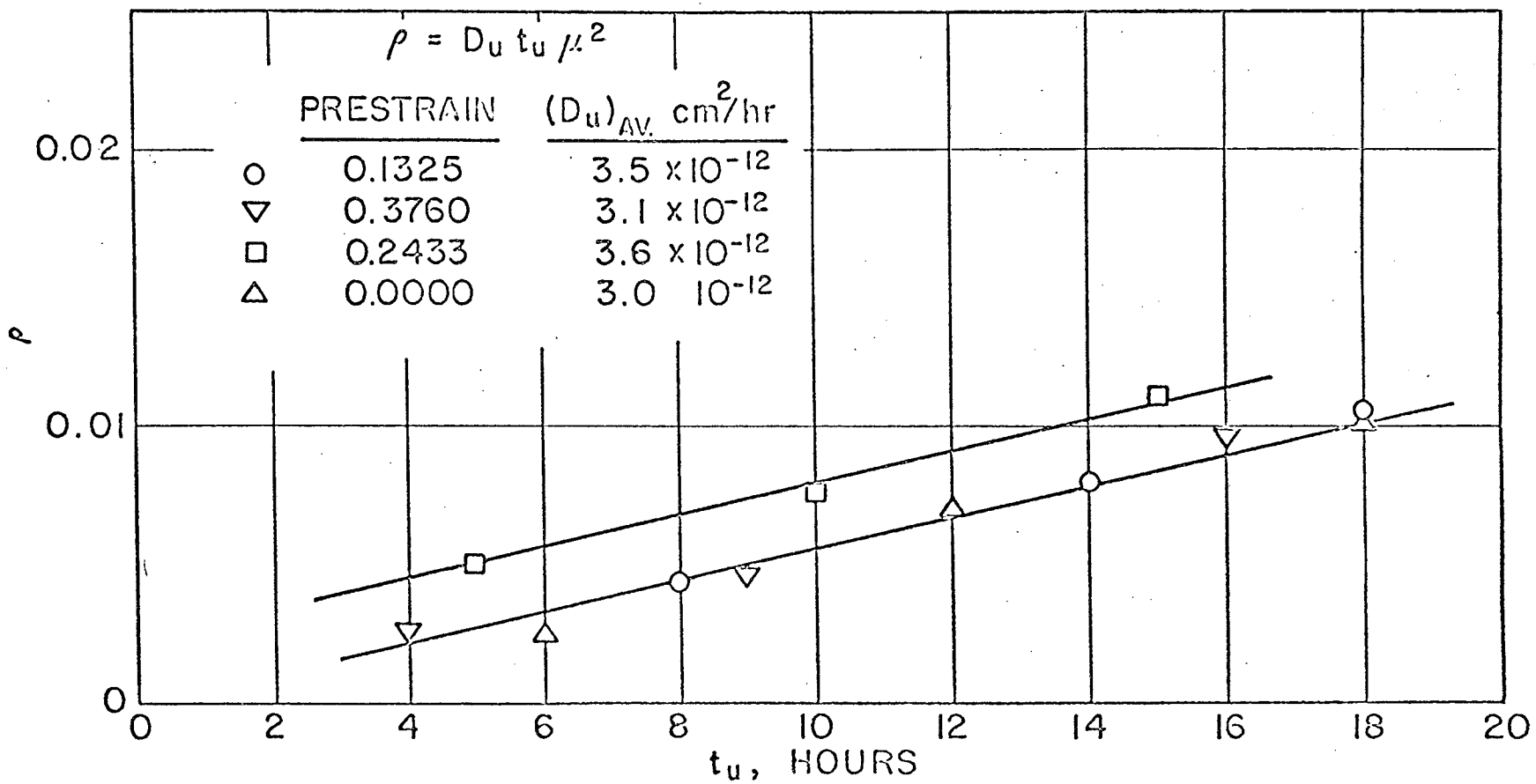

FIG. 6 ρ AS A FUNCTION OF TIME FOR STATIC DIFFUSION ANNEALS OF PRESTRAINED SINGLE CRYSTALS AT 948°K.

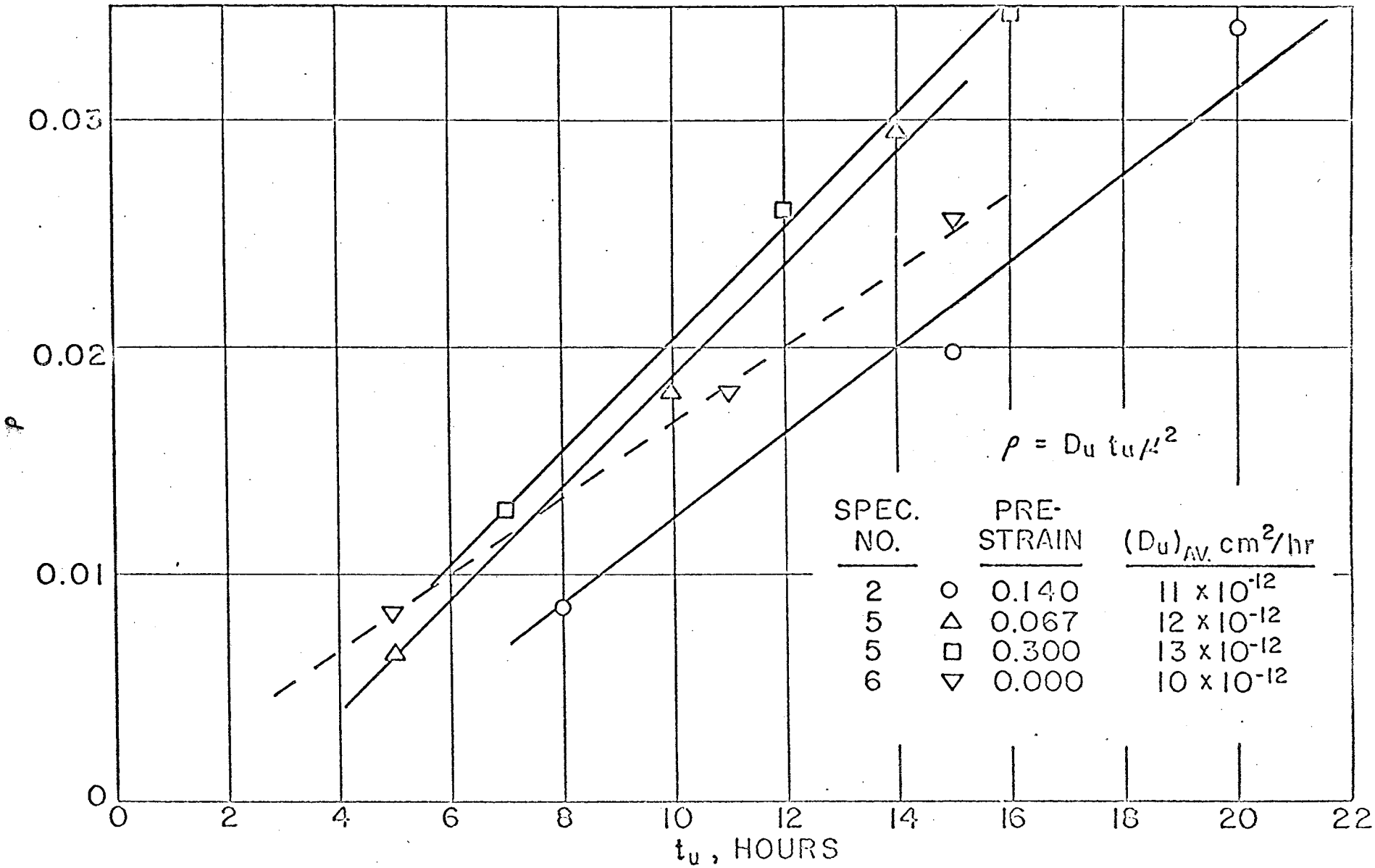

FIG. 5 ρ AS A FUNCTION OF TIME FOR STATIC DIFFUSION ANNEALS OF PRESTRAINED SINGLE CRYSTALS AT 1023°K.

TABLE III -a

Experimental Values of Diffusion Coefficient for Ni Polycrystals (Prestrained)

Specimen	Temp. ^{o}K	Strain	Anneal	t_u (hr)	(I_o/I)av.	ρ av.	(D_u Poly-Crystal) cm^2/hr	(D_u Single Crystal) cm^2/hr
30	1023 ± 1.5^{o}	0.0	1	5	0.8134	.038	46×10^{-12}	15×10^{-12}
			2	"	0.7531	.075	44.5×10^{-12}	
			3	"	0.7092	.114	47×10^{-12}	
31	"	0.047	1	5	0.80917	.0400	48×10^{-12}	15×10^{-12}
			2	"	0.7550	.0738	40×10^{-12}	
			3	"	0.7108	.01130	47×10^{-12}	
64	"	0.131	1	5	0.8051	.0420	50.5×10^{-12}	15×10^{-12}
			2	"	0.7512	.0771	42×10^{-12}	
			3	"	0.7082	.115	57.7×10^{-12}	
33	"	0.251	1	5	0.8049	.042	50.5×10^{-12}	15×10^{-12}
			2	"	0.7464	.081	47×10^{-12}	
			3	"	0.7051	.111	36×10^{-12}	
34	"	0.349	1	5	0.8001	.0450	54×10^{-12}	15×10^{-12}
			2	"	0.7430	.0825	45×10^{-12}	
			3	"	0.7035	.1225	48×10^{-12}	

TABLE III-a continued

Specimen	Temp. ^{o}K	Strain	Anneal	t_u (hr)	(I_o/I)av.	ρ av.	(D_uPoly-crystal) cm^2/hr	(D_uSingle-crystal)* cm^2/hr
40	973 ± 1.5	0.0	1	8	0.8464	0.024	18×10^{-12}	7×10^{-12}
			2	"	0.7802	0.057	25×10^{-12}	
			3	"	0.7465	0.081	18×10^{-12}	
11	"	0.055	1	8	0.8356	0.028	21×10^{-12}	7×10^{-12}
			2	"	0.7852	0.053	18.8×10^{-12}	
			3	"	0.7402	0.085	24×10^{-12}	
22	"	0.151	1	8	0.8454	0.0249	18.7×10^{-12}	7×10^{-12}
			2	"	0.7834	0.055	22.5×10^{-12}	
			3	"	0.7470	0.081	19.5×10^{-12}	
23	"	0.249	1	8	0.8410	0.026	19.5×10^{-12}	7×10^{-12}
			2	"	0.7902	0.050	18×10^{-12}	
			3	"	0.7530	0.074	18×10^{-12}	
24	"	0.360	1	8	0.836	0.028	23×10^{-12}	7×10^{-12}
			2	"	0.772	0.062	25.5×10^{-12}	
			3	"	0.735	0.090	23×10^{-12}	

* Undeformed

TABLE III-a continued

Specimen	Temp. ^{o}K	Strain	Anneal	t_u (hr)	(I_o/I)av.	P av.	(D_uPoly-crystal) cm^2/hr	(D_uSingle-crystal) cm^2/hr
20	948 ± 1.5	0.00	1	7	0.8760	0.0150	13×10^{-12}	
			2	"	0.8332	0.0291	12×10^{-12}	3.5×10^{-12}
			3	6	0.8050	0.0422	13×10^{-12}	
41	"	0.049	1	7	0.8832	0.0130	11×10^{-12}	
			2	"	0.8410	0.0266	11.7×10^{-12}	3.5×10^{-12}
			3	6	0.816	0.0396	13×10^{-12}	
12	"	0.142	1	7	0.8773	0.0145	12.4×10^{-12}	
			2	"	0.8210	0.0351	17.7×10^{-12}	3.5×10^{-12}
			3	6	0.8022	0.0435	8.4×10^{-12}	
13	"	0.230	1	7	0.8713	0.0166	14.24×10^{-12}	
			2	"	0.8220	0.034	15×10^{-12}	3.5×10^{-12}
			3	6	0.792	0.049	15×10^{-12}	
14	"	0.306	1	7	0.8683	0.0171	14.7×10^{-12}	
			2	"	0.8250	0.0325	13.2×10^{-12}	3.5×10^{-12}
			3	6	0.7972	0.0465	14×10^{-12}	

TABLE III - b

Values of Diffusion Coefficient for Prestrained Nickel Single Crystals from Experimental Data

Temp. K	Prestrain	Anneal	t_u (hr)	(I_o/I)av.	ρ av.	$(D_u$ cm^2 / hr) av.
1023	0.000	1	5	0.905	.0082	
1023	0.000	2	6	0.865	.0180	10×10^{-12}
1023	0.000	3	4	0.843	.0255	
1023	0.067	1	5	0.915	.0065	
1023	0.067	2	5	0.866	.0180	12×10^{-12}
1023	0.067	3	4	0.833	.0295	
1023	0.140	1	8	0.904	.0084	
1023	0.140	2	7	0.854	.01970	11×10^{-12}
1023	0.140	3	5	0.822	.0340	
1023	0.300	1	7	0.8840	.01275	
1023	0.300	2	5	0.8421	.0260	13×10^{-12}
1023	0.300	3	4	0.820	.0345	

TABLE III - b (Continued)

Temp. K	Prestrain	Anneal	t_u (hr)	(I_o/I) av.	ρ av.	$(D_u$ cm^2/hr) av.
948	0.000	1	6	0.946	.0025	
948	0.000	2	6	0.913	.0070	3.0×10^{-12}
948	0.000	3	6	0.897	.0100	
948	0.1325	1	8	0.931	.0043	
948	0.1325	2	6	0.907	.0080	3.5×10^{-12}
948	0.1325	3	4	0.893	.0105	
948	0.243	1	5	0.925	.0050	
948	0.243	2	5	0.910	.0075	3.6×10^{-12}
948	0.243	3	5	0.892	.0110	
948	0.3760	1	4	0.945	.0025	
948	0.3760	2	5	0.928	.0045	3.1×10^{-12}
948	0.3760	3	7	0.904	.0095	

Table III-c

Summary of Table IIIa

Temp °K	T^*/T_M	D'_u (polycrystals)$_{av}$ cm^2/hr	D_u (single crystals)$_{av}$ cm^2/hr
1023 ± 1.5	0.591	47×10^{-12}	15×10^{-12}
973 ± 1.5	0.563	20.7×10^{-12}	8×10^{-12}
948 ± 1.5	0.548	13.2×10^{-12}	3.5×10^{-12}

$$D_u(\text{single crystals}) = 1.9 \text{ Exp} \left(- \frac{66,800}{RT} \right) Cm^2/sec.$$

$$D'_u(\text{polycrystals}) = 1.1 \times 10^{-7} \text{ Exp} \left(- \frac{32,300}{RT} \right) Cm^2/sec.$$

* T_M = melting point of nickel, 1728°K.

TABLE III-d

Diffusion Coefficient in Silver after Hoffman and Turnbull (I5)

T/T_m *	D_u (single crystal) cm^2/sec	D_u (fine-grained) cm^2/sec	D_u (coarse-grain) cm^2/sec
$0.627 \leqslant T/T_m \leqslant 0.951$	$D_u = .895\ Exp(-45,950/RT)$		
$0.809 \leqslant T/T_m \leqslant 0.992$			$D_u = .895\ Exp(-45,950/RT)$
$T/T_m \geqslant 0.789$		$D_u = .895\ Exp(-45,950/RT)$	
$0.627 \leqslant T/T_m \leqslant 0.789$		$D_u' = 2.3 \times 10^{-5}\ Exp(-26,400/RT)$**	

* T_m = melting point of silver, $1233.5^{\circ}K$

** $D_u / D_u' = 2$ to 6

discussed in previous section. However, D_s was determined by introducing the values of I_o/I obtained for the dynamic anneals into Eqn. (21) and calculating the corresponding P values. The values of P were then introduced into Eqn. (22) and the corresponding values of D_s were obtained directly. Plots of P vs. t are shown in Figs. 7, 8, 9, and 10. Table IV lists the experimental and calculated results.

Sources of error:

Several sources of scatter and error are inherent in the techniques that were employed. Back reflection Laue radiograms revealed that each specimen was somewhat differently oriented and exhibited differences in sub-structure. Perhaps some of the scatter in is attributable to these factors. The adoption of a series of anneals with the initial heating, cooling and reheating cycles may have resulted in introducing some errors. Estimates using the experimentally obtained diffusivities, however, suggest that practically no error was introduced from this source. Undoubtedly, the greatest source of error arises from a possible error in the value of μ used in this investigation. On the other hand it is difficult to visualize that this factor can introduce more than about a uniform 16% error in the calculated diffusivities. The correlation between D_u obtained in this investigation and the values previously obtained by other investigators, as shown in Fig. 11, is rather good and attest to the nominal validity of the procedures employed.

Results

I. Prestrained Single and Polycrystals Results.

For purposes of discussion the values of the diffusion coefficient, in prestrained and in undeformed single and polycrystalline nickel specimens, over the temperature range of 675 C to 750 C and for total

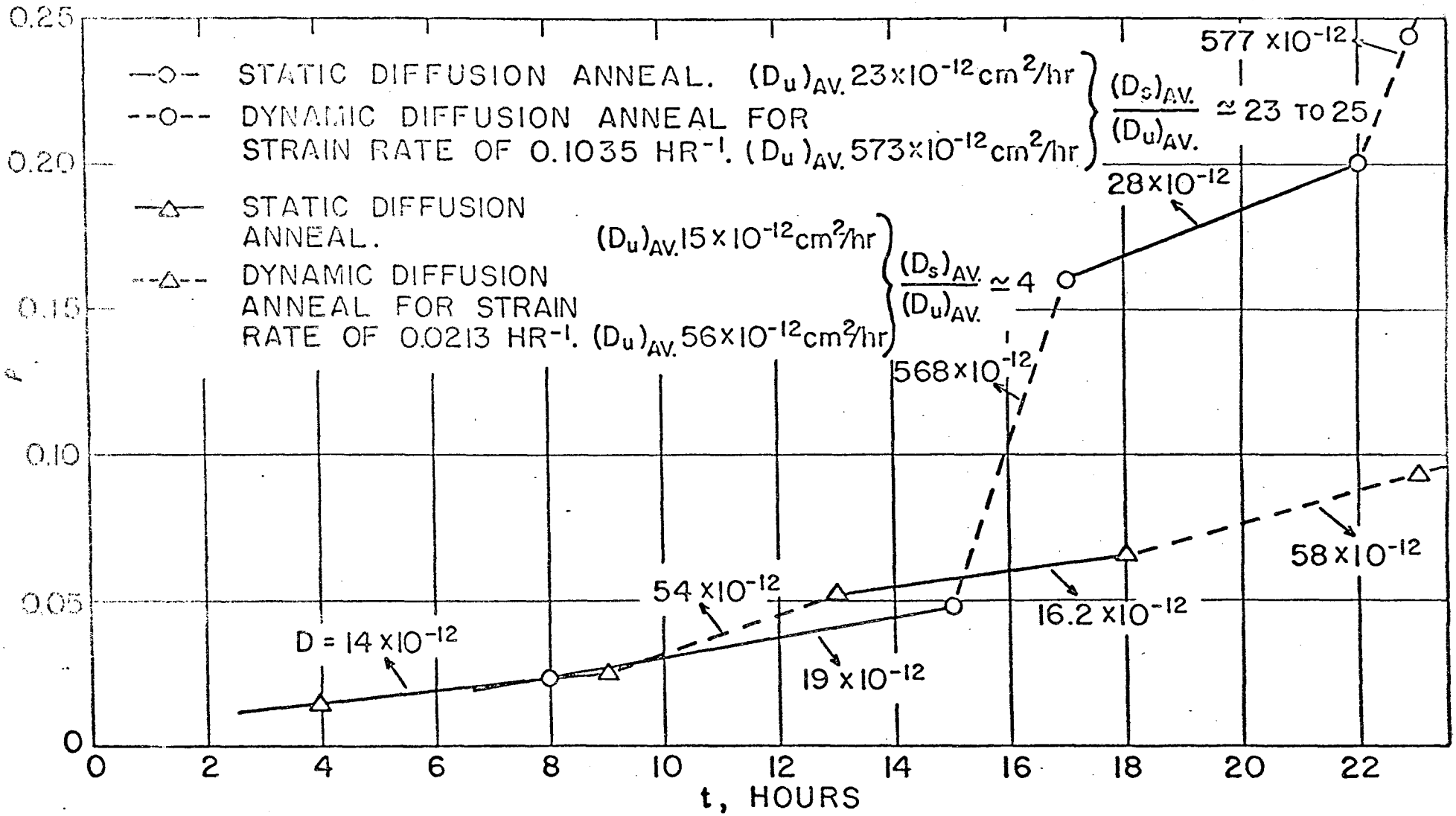

FIG. 7 ρ AS A FUNCTION OF TIME FOR STATIC AND DYNAMIC DIFFUSION ANNEALS AT 1023 °K.

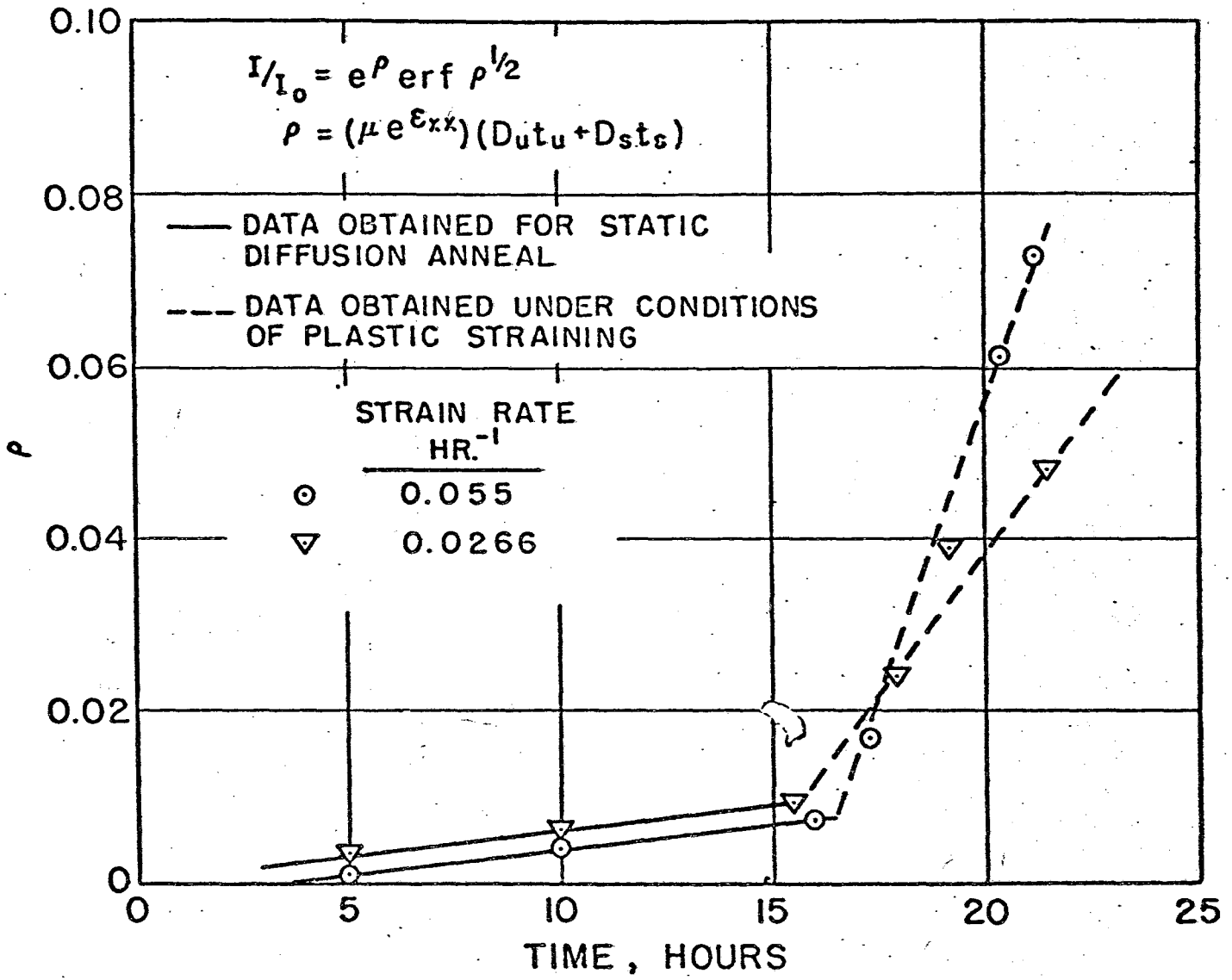

FIG. 8 ρ AS A FUNCTION OF TIME FOR A STATIC AND DYNAMIC DIFFUSION ANNEAL AT 948 °K.

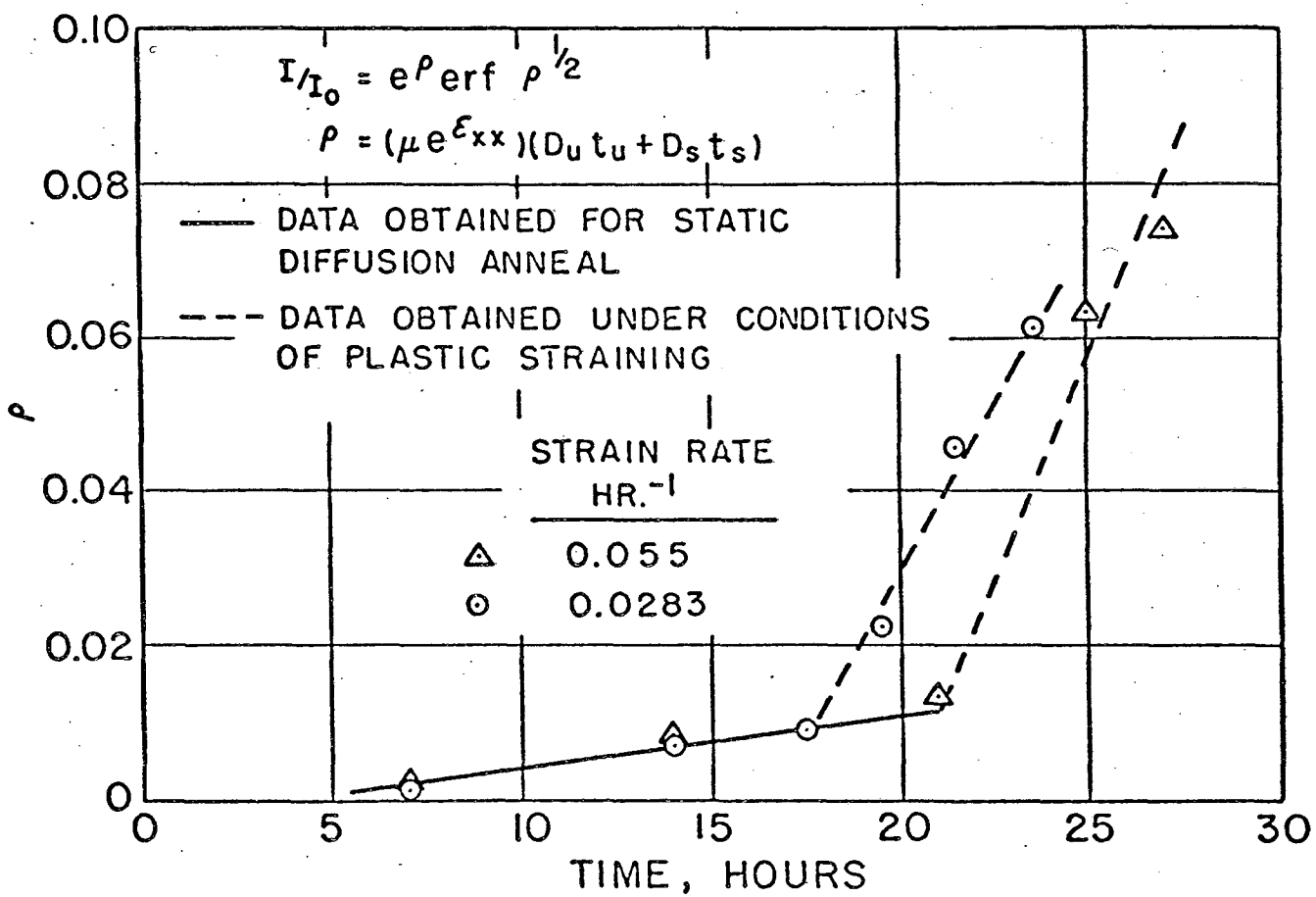

FIG. 9 ρ AS A FUNCTION OF TIME FOR A STATIC AND DYNAMIC DIFFUSION ANNEAL AT 973 °K.

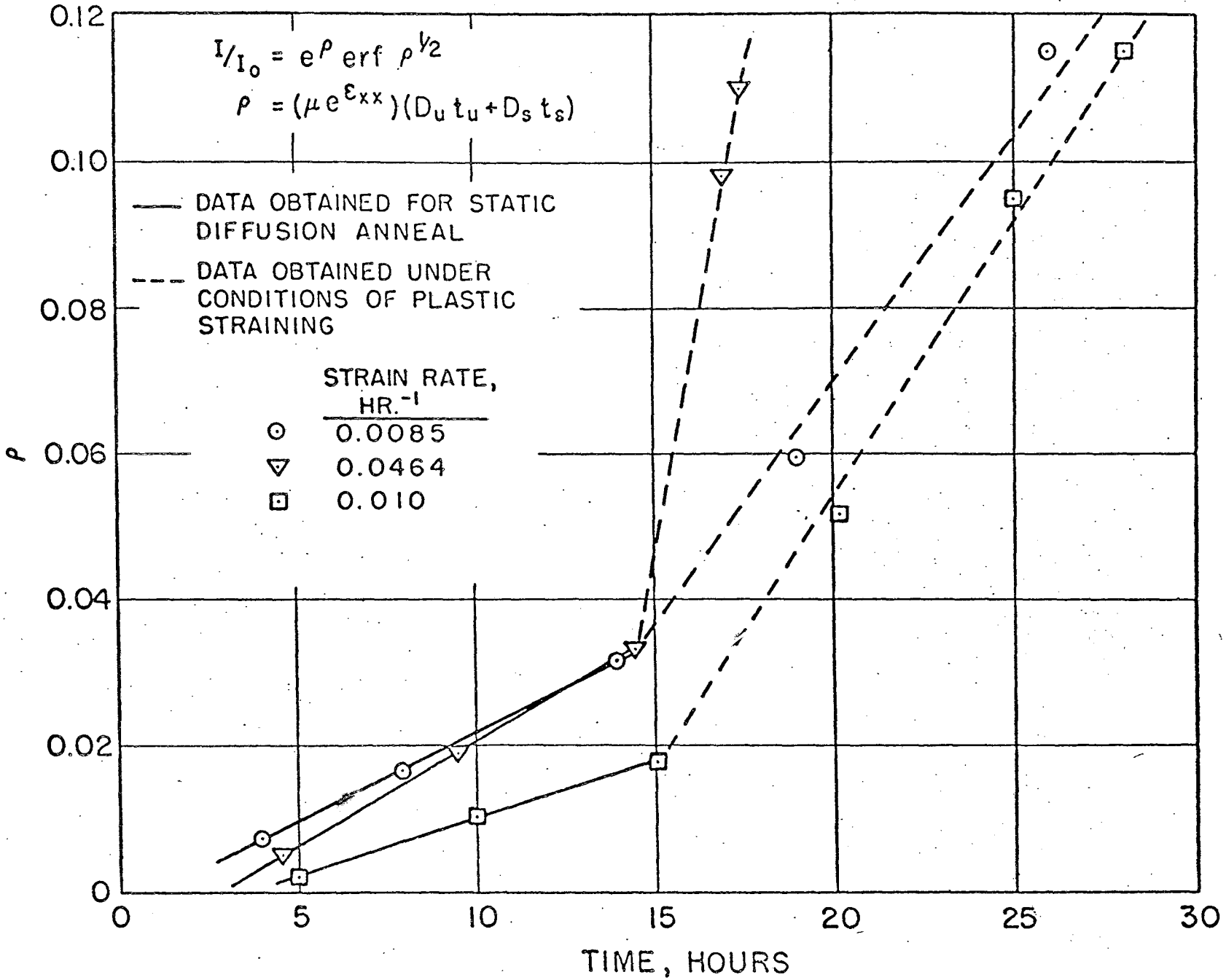

FIG. 10 ρ AS A FUNCTION OF TIME FOR A STATIC AND DYNAMIC DIFFUSION ANNEAL AT 1021 °K.

TABLE I V-b

Values of Diffusivity Calculated from Experimental Data

Specimen	Temp. ^{o}K	Anneal	t_u(hr)	t_s(hr)	I/I_o(av.)	ρ	ε_{zz}	ε_{xx}	$\gamma_{II}hr^{-1}$	$D_s cm^2/hr$ *
1	1021 + 1.5	1	5	0	.952	.002	0	0	.01	$.97 \times 10^{-11}$
	"	2	5	0	.898	.010	0	0	"	"
	"	3	5	0	.865	.018	0	0	"	"
	"	4	1/4	5 1/2	.788	.051	.0671	-.0307	"	3.3×10^{-11}
	"	5	1/4	4 1/2	.729	.095	.1185	-.0543	"	4.9×10^{-11}
	"	6	1/4	3 1/2	.707	.115	.1349	-.0618	"	4.7×10^{-11}
2	"	1	4	0	.913	.007	0	0	.0085	1.46×10^{-11}
	"	2	4	0	.870	.017	0	0	"	"
	"	3	6	0	.827	.032	0	0	"	"
	"	4	1	4	.773	.059	.0459	-.035	"	4×10^{-11}
	"	5	1/4	7	.708	.115	.0882	-.072	"	5.1×10^{-11}
3	"	1	4 1/2	0	.923	.005	0	0	.0464	2.15×10^{-11}
	"	2	5	0	.861	.019	0	0	"	2.14×10^{-11}
	"	3	5	0	.824	.033	0	0	"	"
	"	4	1/2	2 1/2	.725	.098	.1157	-.0912	"	15.3×10^{-11}
	"	5	1/2	1/2	.713	.110	.1324	-.104	"	16.2×10^{-11}

continued on next page

TABLE IV - b (Continued)

Values of Diffusivity Calculated from Experimental Data

Specimen	Temp. K	Anneal	t_u(hr)	t_s(hr)	I/I_o(av.)	ρ	E_{zz}	E_{xx}	γ hr^{-1}	D_s cm^2/hr*
6	973	1	7	0	0.960	.00135	0	0	0	6.0×10^{-12}
	"	2	7	0	0.910	.0073	0	0	0	"
	"	3	3.5	0	0.898	.0096	0	0	0	"
	"	4	0	2	0.850	.0227	.07	-.05	.0283	37×10^{-12}
	"	5	0	2	0.797	.0460	.113	-.09	"	59×10^{-12}
	"	6	0	2	0.770	.0615	.170	-.12	"	58×10^{-12}
7	"	1	7	0	0.956	.0017	0	0	0	6.5×10^{-12}
	"	2	7	0	0.906	.0080	0	0	0	"
	"	3	7	0	0.879	.0140	0	0	0	"
	"	4	0	4	0.769	.0635	0.22	-.16	.053	115×10^{-12}
	"	5	0	2	0.742	.0830	0.305	-.21	"	108×10^{-12}

*$D_s = D_u$ for $E_{zz} = 0$

TABLE IV-b Continued

Specimen	Temp. °K	Anneal	t_u(hr)	t_s(hr)	I/I_o(av.)	ρ	ε_{zz}	ε_{xx}	$\dot{\gamma}_{II}$ hr^{-1}	D_s cm^2/hr *
4	948 ± 1.5	1	5	0	.960	.001	0	0	.005	3.5×10^{-12}
	"	2	5	0	.930	.004	0	0	"	"
	"	3	6	0	.905	.008	0	0	"	"
	"	4	1/4	1/2	.865	.017	.816	-.054	"	38.6×10^{-12}
	"	5	1/4	3	.770	.062	.264	-.176	"	105×10^{-12}
	"	6	1/4	1 1/4	.755	.073	.319	-.213	"	107×10^{-12}
5	"	1	5	0	.942	.003	0	0	.0266	3.55×10^{-12}
	"	2	5	0	.920	.006	0	0	"	"
	"	3	5 1/2	0	.890	.009	0	0	"	"
	"	4	1/4	2.55	.846	.024	.066	-.062	"	42.7×10^{-12}
	"	5	1/4	2	.813	.039	.102	-.095	"	50.1×10^{-12}
	"	6	1/4	2 1/4	.787	.048	.163	-.152	"	49.3×10^{-12}

*$D_s = D_u$ for $\varepsilon_{xx} = 0$

TABLE IV - b

Values of Diffusion Coefficient for Single Crystals given Cyclic Static-Dynamic Diffusion Anneals

Specimen	Temp, K	Anneal	t_u(hr)	t_s(hr)	(I_o/I) av.	ρ av.	$\dot{E}$ hr^{-1}	$\dot{E}_{zz}$	D cm^2/hr
1	1023	1	8	0	0.845	0.0245	0.	0.	23×10^{-12}
	1023	2	7	0	0.795	0.0474	0.	0.	23×10^{-12}
	1023	3	0	2	0.672	0.1600	0.1035	0.207	568×10^{-12}
	1023	4	5	0	0.642	0.200	0.	0.207	28×10^{-12}
	1023	5	0	1	0.618	0.244	0.1035	0.310	577×10^{-12}
2	1023	1	4	0	0.879	0.014	0.	0.	14×10^{-12}
	1023	2	5	0	0.842	0.026	0.	0.	14×10^{-12}
	1023	3	0	4	0.787	0.053	0.02	0.08	54×10^{-12}
	1023	4	5	0	0.765	0.065	0.	0.08	16.2×10^{-12}
	1023	5	0	5	0.730	0.094	0.021	0.193	58×10^{-12}

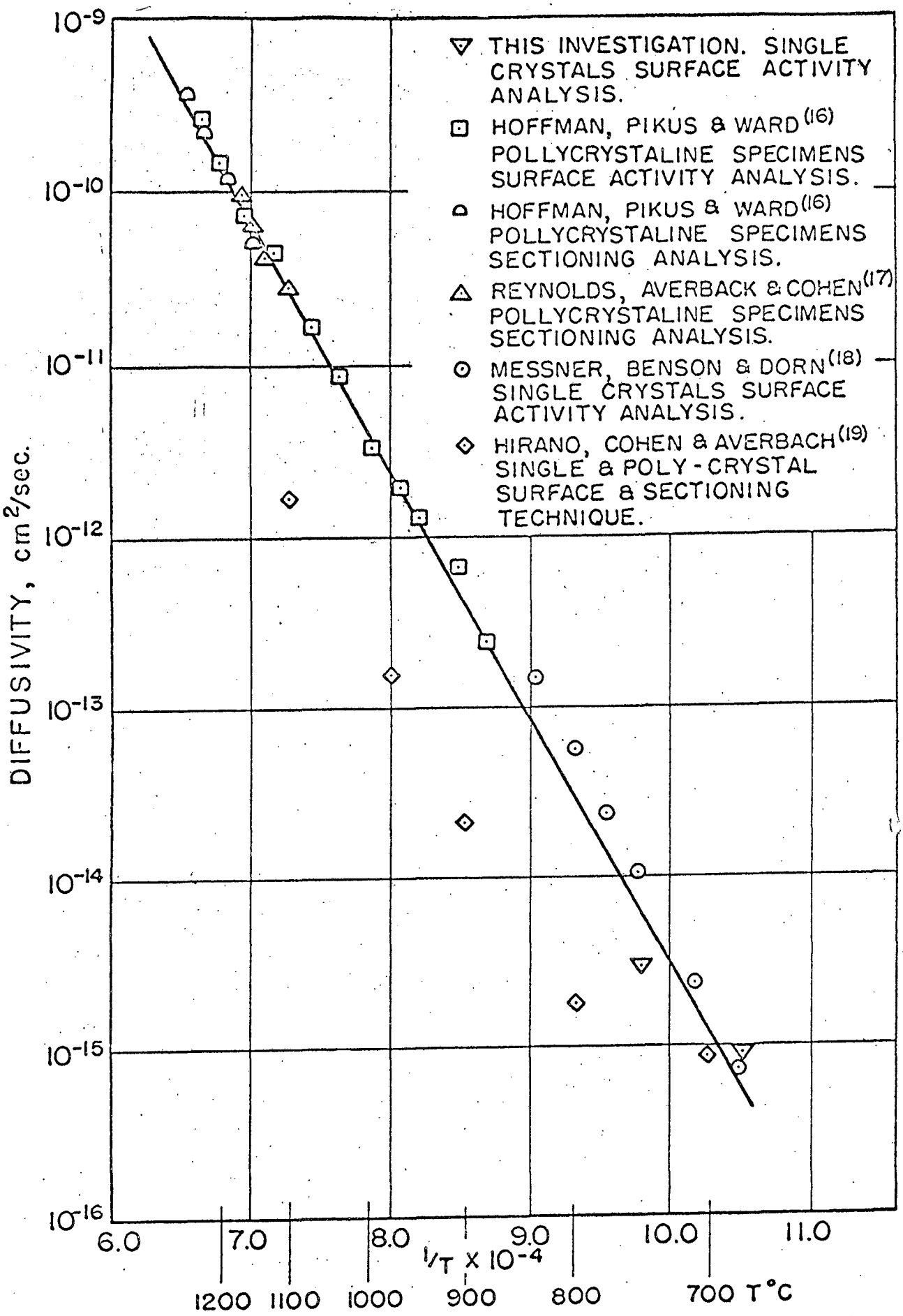

FIG. 11 TEMPERATURE DEPENDENCE OF SELF DIFFUSIVITY IN NICKEL.

strains of 0.32 to 0.00, are given in tables III a and III b correspondingly. These data although somewhat scattered, clearly reveal that the diffusivity in single and polycrystalline specimens is independent of their mechanical history (strain, strain rate, etc.) However, it is clear that the diffusion coefficient in a fine-grained crystal, D'_u, is larger than that of the single crystal, D_u, at the same temperature provided that the ratio $T/T_m \leqslant 0.60$ holds, where T is the annealing temperature and T_m the melting point, °K.

Table (IIIc) shows that the apparent self-diffusion coefficient, D'_u, is larger than D_u, by a factor of 2 to 4 and is represented by the equation:

$$D_u = I.I\ (I0)^{-7} \exp\ (-32{,}300/RT\ )\ Cm^2\text{-}Sec^{-I} \qquad (25)$$

The ratio D'_u/D_u being larger for the lower temperatures. These results are in qualitative agreement with those of Hoffman and Turnbull[15] as shown in table III d.

Whether or not the apparent coefficient, D'_u, differs from the lattice diffusion coefficient, D_u, depends on the ratio of the absolute grain-boundary diffusion coefficient, D_{gb}, to the lattice diffusion coefficient [20] D_u. Turnbull has shown that D'_u will not differ from D_u appreciably unless $D_{gb}/D_u > N$ where N is a number larger than unity and is a function of the grain size. In view of the widely accepted fact that the activation energy for grain boundary diffusion is less than that for volume diffusion, it becomes self-evident that D_{gb}/D_u and hence D'_u/D_u must increase with decreasing temperature. This observation is inqualitative harmony with the results listed in table III C.

The D'_u values presented in table III C are not the absolute grain boundary diffusion coefficients. (It is commonly accepted that

$D_{gb}/D_u \approx 10^7$) And it is not clear whether or not the activation energy, 32,300 Cal/mole is that of grain-boundary self diffusion. Fisher[21] has analyzed the problem of grain boundary diffusion making use of penetration curves. However, since our data was obtained by a surface counting technique, it was not possible to use Fisher's analysis, without the aid of arbitrary assumptions, to calculate the absolute values of D_{gb} and the corresponding grain-boundary activation energy.

II. Dynamically Annealed Single Crystals results and the effect of strain rate on the diffusion coefficient.

For purposes of discussion, values of $\bar{D}_s/D_u$ that were obtained in this and earlier (authors master thesis, University of California, 1961) investigations are presented in table V as a function of temperature and strain rate. Also the calculated values of $\frac{1}{\dot{\xi}}(D_s - D_u)$ and $(\bar{D}_s - D_u)$ are plotted as a function of time and strain rate, figures I2a and 13 respectively.

The results presented in table V, Figs. 12a and 13 are in qualitative agreement with the results of several other investigators as shown in table I and Figs. 14 and 15.

The diffusion coefficient of the dynamically annealed crystals D_s increases with time up to a steady state value D_s (see Fig. 12b) which is almost linearly dependent on the strain rate at a constant temperature.

These data can be summarized as follows:

$$\frac{D_s}{D_u} = 1 + 230 \qquad \text{at } T = 1021 \text{ K} \qquad (26)$$

$$= 1 + 392 \qquad \text{at } T = 973 \text{ K} \qquad (27)$$

$$= 1 + 510 \qquad \text{at } T = 948 \text{ K} \qquad (28)$$

TABLE V

Steady State Values of $\bar{D}_s/D_u$

Metal	Temp.°K	Strain Rate hr^{-1}	$\bar{D}_s/D_u$
Ni	1021	0.1035	23
"	"	0.0464	8
"	"	0.0210	4
"	"	0.0100	3
"	973	0.0530	22
"	"	0.0283	12
"	948	0.0550	30
"	"	0.0266	14

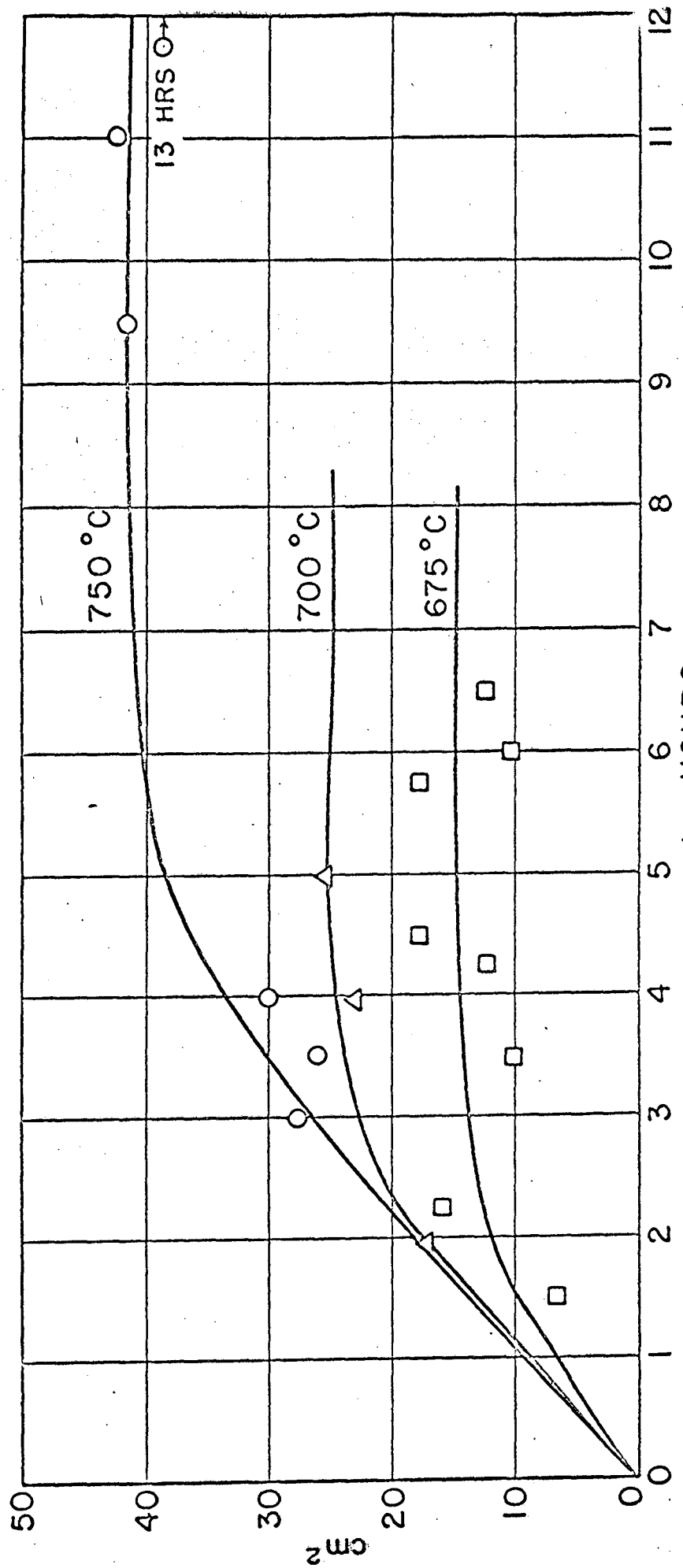

FIG. 12a A PLOT OF $\left(\frac{\int_0^{t_s} D dt_s}{t_s} - D_u\right) \frac{1}{\dot{\varepsilon}} \times 10^{10}$ vs. t_s.

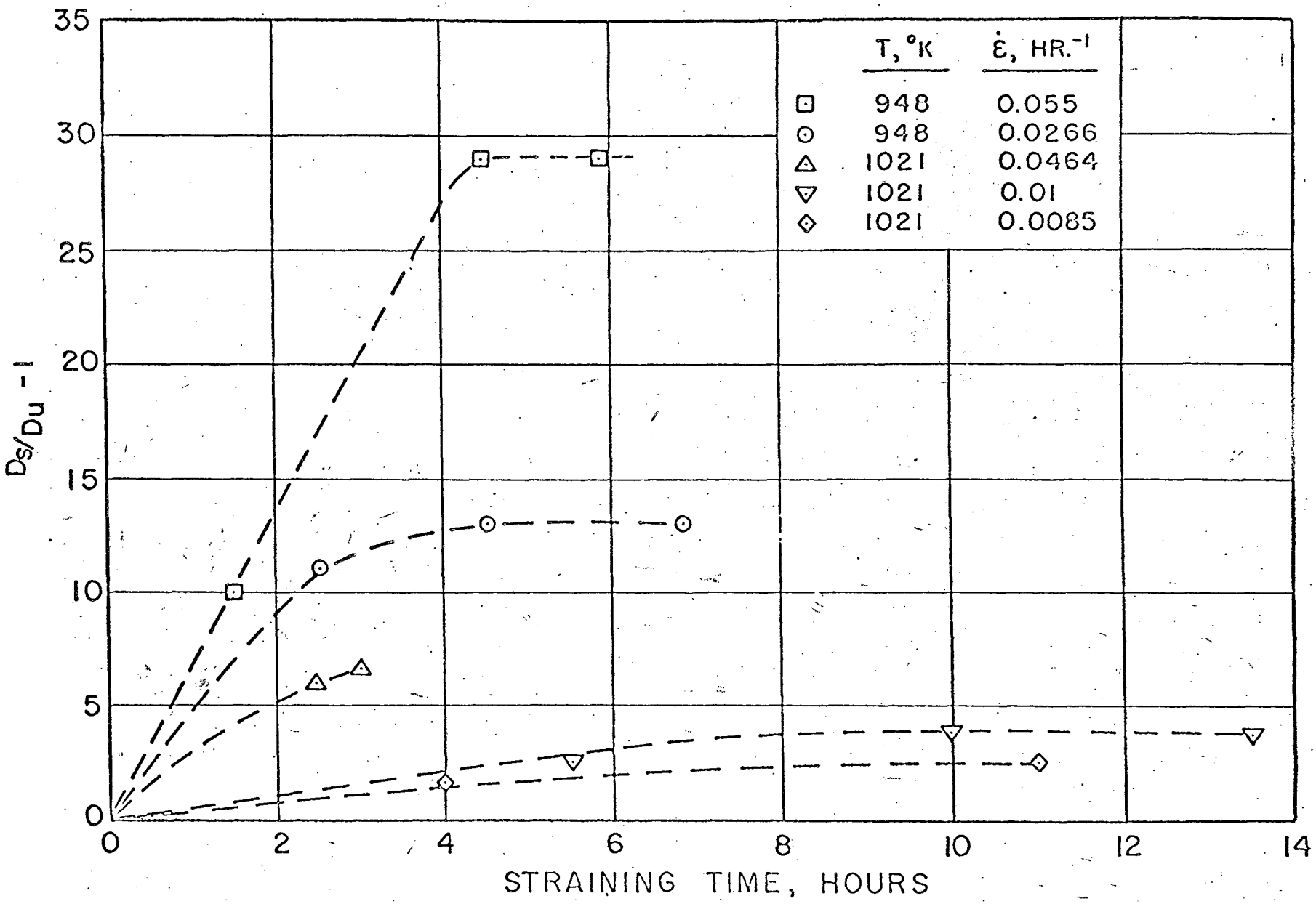

FIG. 12b THE RATIO OF THE DIFFUSION COEFFICIENT IN STRAINED NICKEL TO THE DIFFUSION COEFFICIENT IN UNSTRAINED NICKEL vs. THE STRAINING TIME AT VARIOUS STRAIN RATES AND TEMPERATURES.

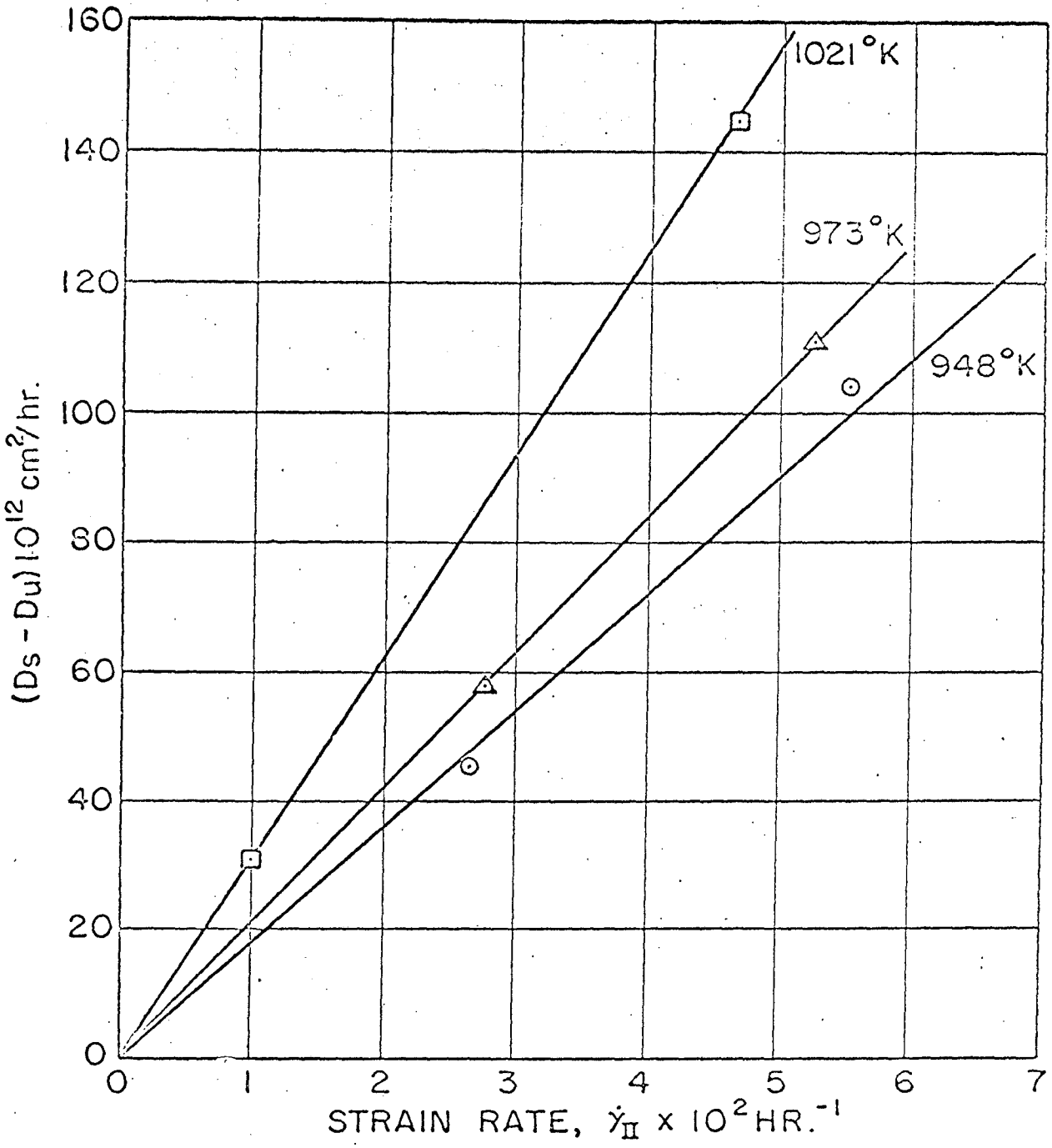

FIG. 13 THE DIFFERENCE IN DIFFUSION COEFFICIENTS IN STRAINED AND UNSTRAINED NICKEL vs. THE STRAIN RATE $\dot{\gamma}_{II}$, FOR VARIOUS TEMPERATURES.

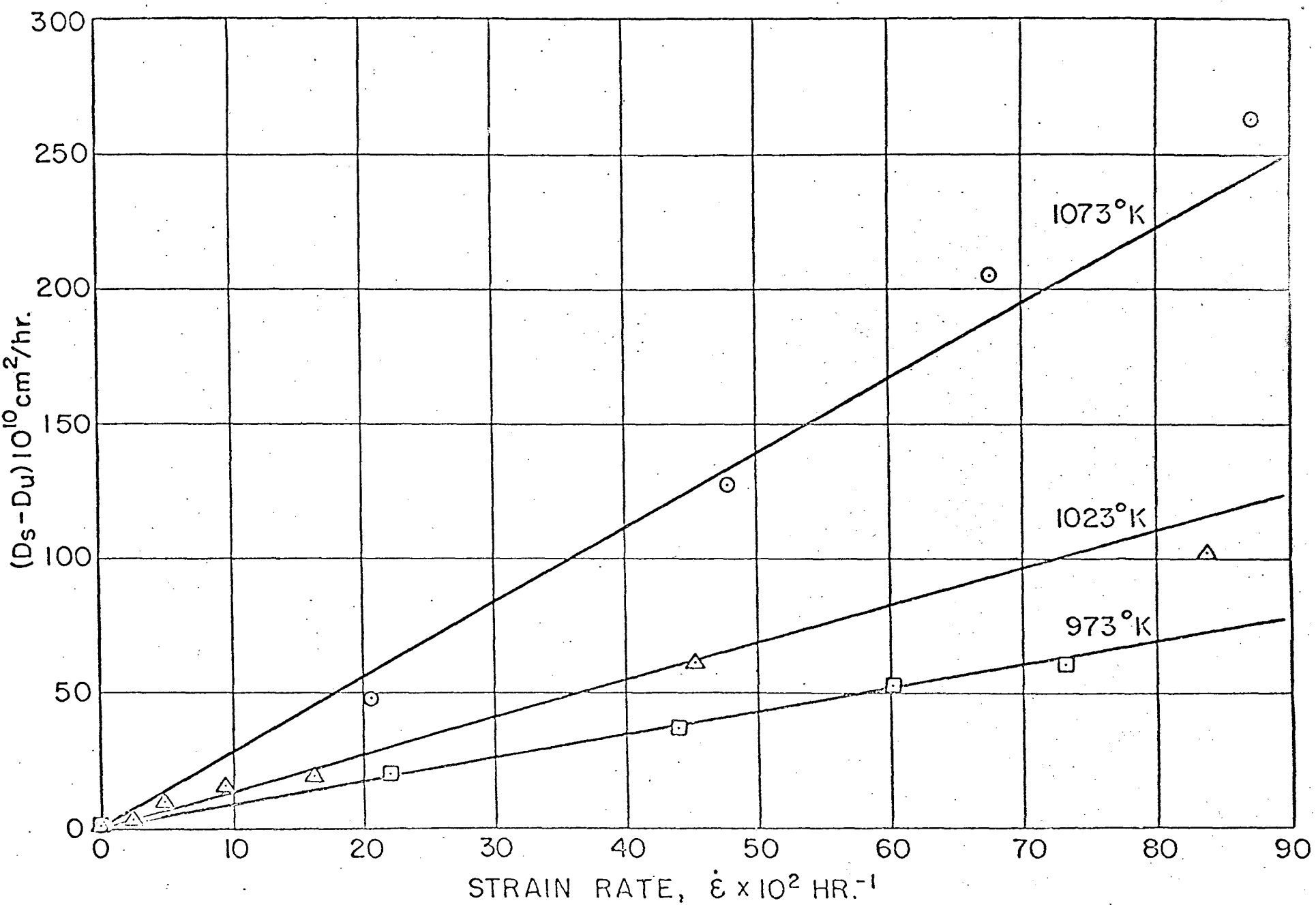

FIG. 14. THE DIFFERENCE IN DIFFUSION COEFFICIENTS IN STRAINED AND UNSTRAINED SILVER vs. THE STRAIN RATE FOR VARIOUS TEMPERATURES. (AFTER LEE & MADDIN)

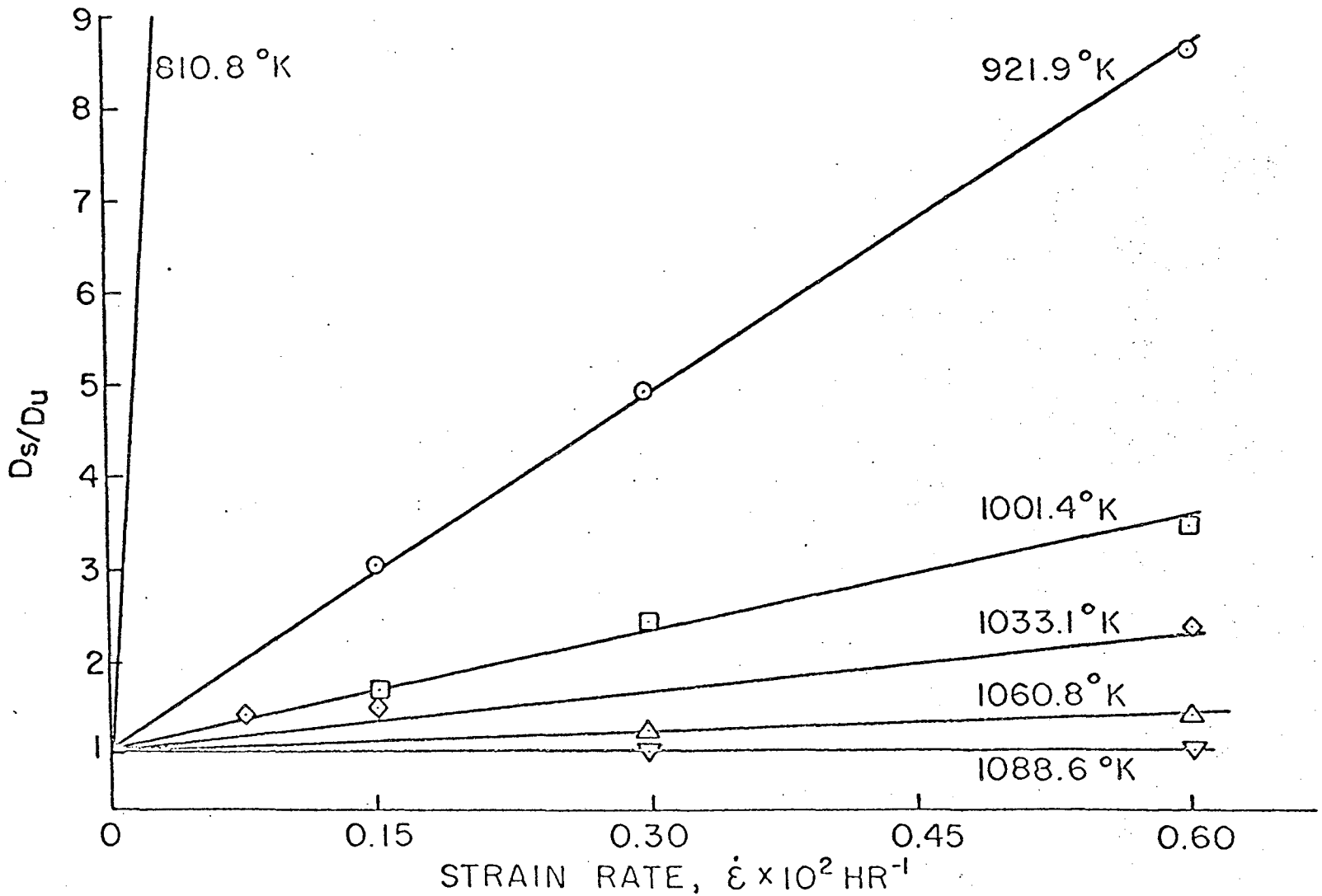

FIG. 15 THE RATIO OF THE DIFFUSION COEFFICIENT IN STRAINED SILVER TO THE DIFFUSION COEFFICIENT IN UNSTRAINED SILVER vs. THE STRAIN RATE AT VARIOUS TEMPERATURES. (AFTER GIRIFALCO & FORESTIERI)

DISCUSSION

In view of the present incomplete theoretical understanding of all pertinent details and in view of the limited data currently available, a definitive analysis of the enhanced diffusivity that is obtained under conditions of plastic straining will not be attempted here. Nevertheless, it may be worthwhile to set down some tentative ideas on this subject.

Several different factors might contribute to the enhancement of the diffusivity under plastic straining. For example, (1) increase in the interstitial diffusivity, (2) increase in the vacancy diffusivity, and (3) short circuiting along dislocations.

I. Interstitial diffusion:

Excess interstitials may be formed during plastic deformation as a result of motion of interstitial forming jogs which would lead to an increase in the interstitialcy diffusivity. However, Hirsh[22] has stated that interstitial forming jogs can migrate conservatively to nodal points so that little if any enhanced diffusivity is to be expected from the interstitialcy mechanism. Furthermore, some evidence from data on the production of point defects at lower temperatures indicates that mostly vacancies are introduced rather than interstitials.[23] This latter observation is consistent with energy considerations since the energy to form an interstitial is greater than the energy to form a vacancy.

II. Vacancy diffusion:

For a system undergoing diffusion via the vacancy mechanism the diffusion coefficient is given by:

$$D_u = D_v \sqrt{\nu}\, n_o \qquad (29)$$

where D_u = the self-diffusion coefficient in unstrained lattice,

D_v = the diffusivity of a vacancy

Ω = the atomic volume and

n_o = the equilibrium number of vacancies

Hence the introduction of excess vacancies upon plastic straining leads to an enhanced diffusivity D_s,

$$D_s = D_v \Omega (n_o + n_x) \tag{30}$$

Where

n_x = the average excess number of vacancies.

Two different mechanisms can contribute to the formations of vacancies during creep. First, the motion of vacancy producing jogs and second, the climb of edge dislocations (see appendix II). Undoubtedly, the deformation and hence the formation of vacancies is controlled by both the glide of jogged screw dislocations and the climb of edge dislocations. The resulting creep rate when both mechanisms are operating simultaneously may be written as the same of two terms:

$$\dot{E}_{total} = \dot{E}_j + \dot{E}_c \tag{31}$$

where

$\dot{E}_j$ = the creep rate due to the motion of vacancy producing jogs,

$\dot{E}_c$ = the creep rate due to the climb of edge dislocations.

If we assume that the rate of disappearance of excess vacancies (at dislocations) for unit volume be proportional to their concentration, then the steady state net excess number of vacancies n_x produced during straining is related to the strain rate as follows (see appendix II for detailed derivation):

$$\bar{n}_x = L^2/4D_v \, (h \dot{E}_c/L_I \, b^3 + p \dot{E}_j/l_j \, b^2) \tag{32}$$

When Eqns. (30 and 32) are combined, one finally obtains the following expression for the steady state diffusivity in a crystal undergoing plastic straining:

$$\bar{D}_s = D_v + \left[\frac{1.5 \sqrt{2} L^2 h (1-\mu)^4 \pi^4 Z N_s^2 \tau^5}{L_1 P_s b^9 G^4 k_2 T \sinh\left(\frac{\tau l_j b^2 / P_s}{k_2 T}\right)} e^{-q_j''/k_2 T} \right] \dot{\varepsilon} \qquad (33)$$

The above equation shows that the enhanced diffusion coefficient, $\bar{D}_s$, is linearly dependent on the strain rate. Although this observation is in qualitative agreement with the experimental data presented in Fig. 12, we shall attempt next to show that it does not seem possible for the motion of jogged screws or climbing edge dislocations to produce the number of vacancies that is required to account for the observed enhancement in the self-diffusivity.

A maximum steady state enhancement of about thirty times was observed at the temperature 948°K and for a strain rate of 0.055 hr^{-1}. Equation (30) which is repeated here may be used to estimate the steady state vacancy concentration that would account for this enhancement.

$$D_s = D_v \sqrt{\nu} (n_0 + n_{1x}) = \frac{a^2}{12} \left(\frac{n_0}{n_s} + \frac{n_{1x}}{n_s} \right) \quad \text{(For FCC metals)} \qquad (30\text{-a})$$

Where

ν = the vacancy jump frequency

a = the lattice constant

n_s = the number of atomic sites per unit volume.

Assuming that excess vacancies are produced at a uniform rate,

$$\frac{dn^+}{dt} = \frac{N}{t} \qquad (34)$$

Where N = the number of vacancies produced in time t. And that excess vacancies disappear at a rate proportional to their concentration,

$$\frac{dn^-}{dt} = \frac{n_x}{t} = \frac{n_x \nu}{W} \qquad (35)$$

Where

W = the vacancy life time number of jumps

Setting $\frac{dn^+}{dt} = \frac{dn^-}{dt}$ at steady state one obtains

$$\nu \bar{n}_x = \frac{N}{t} W \tag{36}$$

Combining Eqns. (30a and 36) we obtain the following expression for N W

$$(\bar{D}_s - D_u) \frac{12\, t\, n_s}{a^2} = N W \tag{37}$$

For the conditions of our maximum enhancement ($\bar{D}_s = 30\, D_u$, T = 948 K, t_s = 4.5 hours, and E = 26%) one obtains the following value for N W.

$$N W = 2 \times 10^{29} \text{ vacancy jumps}$$

At the present no estimates on the value of W for nickel at high temperatures has been reported in the literature. However, annealing sutdies of quenched-in vacancies near room temperature[24] indicates that the life-time number of jumps is 10^{10} or less. Since the dislocations density, which acts as vacancy sinks, increases with deformation a value of $W = 10^9$ should be a conservative upper limit at the conditions of our experiments. Corresponding to this value of W, N attains the value, $N = 8 \times 10^{18}$ vacancies per cm^3 per 1% strain. This number is about 7 orders of magnitude higher than the equilibrium number for the same temperature. On the basis of current understanding of the motion of jogged screws and the climb of edge dislocations[25] it is highly unlikely that moving dislocations can generate and maintain the steady state concentration of 8×10^{18} vacancies per cm^3 per 1% strain.

III. Short Circuiting:

The previous discussion on the effect of vacancies and interstitials formation during plastic deformation leads to the conclusion that the major factor responsible for the enhancement of the diffusivity upon plastic straining appears to arise from short circuiting along dislocations.

The possibility of diffusion short circuiting along grain

boundaries and dislocations has been the subject of investigation by several authors (15, 21, 26, 27). These investigations lead to the conclusions that (1) the diffusivity along grain boundaries is several orders of magnitude higher than the lattice diffusivity and the activation energy for grain boundary diffusion is about 0.45 the activation energy for lattice diffusion. Second, the edge-type dislocation-pipe diffusivity is at least as large as that of grain boundary diffusion and possibly even larger than the latter.

In view of the fact that no enhanced diffusion was observed in either of the cold worked single or polycrystals, yet a large enhancement was obtained for the dynamically diffused single crystals, it would be reasonable to assume that the enhancement is associated with moving dislocations. This is indeed to be expected since the concentration of vacancies along moving dislocations may temporarily exceed the equilibrium concentration, the vacancies concentration per unit volume remaining almost constant, thus leading to a rapid short circuiting along the moving dislocations. Hence the density of moving dislocations has a great effect on the diffusion coefficient.

The effective diffusion coefficient, D_{eff}, under conditions of plastic straining will be the sum of the fraction of diffusion that takes place along the moving dislocations plus the fraction of diffusion that occurs in the lattice;

$$D_{eff} = D_p f + D_u (1 - f) \qquad (38)$$

Where

f = the fraction of diffusion along the moving dislocations
D_u = the lattice diffusion coefficient
D_p = the diffusion coefficient along moving dislocations.

Table VI gives an estimate of the enhanced diffusivity D_s/D_u due to short circuiting along dislocation pipes using Eqn. 38 and values of f as calculated in appendix III.

TABLE VI.

Estimates of enhanced diffusion, D_s/D_u (based on Eqn. 43) expected for different dislocation densities, p.

Nickel

	D_s/D_u			
Temp. C	$p = 10^6$	10^7	10^8	10^9
750	1	10	100	1,000
700	2.4	24	240	2,400
675	4.3	43	430	4,300

Silver

Temp. C	$p = 10^6$	10^7	10^8	10^9	10^{10}
1,000	5×10^{-4}	5×10^{-3}	5×10^{-2}	5×10^{-1}	5
900	1.35×10^{-3}	1.35×10^{-2}	1.35×10^{-1}	1.35	13.5
800	4×10^{-3}	4×10^{-2}	4×10^{-1}	4	40
700	1.63×10^{-2}	1.63×10^{-1}	1.63	16.3	163
600	9.9×10^{-2}	9.9×10^{-1}	9.9	99	990
500	8×10^{-1}	8	80	800	
400	13	130	1300		

Hart,[28] estimated that f is equal to the fraction of atoms that are in dislocations. Thus, f is linearly dependent on the density of moving dislocations (see appendix III),

$$f = K_1 P \tag{39}$$

where

P = the density of moving dislocations

K_1 = a constant

The pipe diffusivity D_p is linearly dependent on the number of vacancies in the pipe. And we shall assume that the number of vacancies along the moving dislocations slightly exceeds the equilibrium number that exists in the bulk of the material and is proportional to the velocity of jogs on the dislocations and hence to the dislocations velocity itself. Thus one can write for D_p

$$D_p = K_2 \, b \, \upsilon \, e^{-\Delta H_p / RT} \tag{40}$$

where

υ = the dislocations velocity cm/sec

ΔH_p = the activation energy for pipe diffusion

b = the Burgers vector cm, and

K_2 = a numerical constant

Combining Eqns. (38, 39 and 40) and taking (1 - f), one obtains the following expression for D_{eff}

$$D_{eff} = K_2 K_1 P b \upsilon \, e^{-\Delta H_p / RT} + D_u \tag{41}$$

For high temperature creep, one can write for the creep rate

$$\dot{E} = P b \upsilon \tag{42}$$

Where

P, b and ν are as before.

Combining Eqns. (41) and (42) we obtain the final expression for D_{eff}

$$D_{eff} - D_u = K e^{\frac{-\Delta H_p}{RT}} \dot{\varepsilon} \qquad (43)$$

Where

$$K = K_1 K_2$$

A plot of $(D_{eff} - Du) \frac{1}{\dot{\varepsilon}}$ Vs. Temperature is shown in Fig. 16.

Eqn. (43) shows that for a constant temperature the observed diffusion coefficient under conditions of plastic straining increases linearly with the strain rate, a fact that is in excellent agreement with our experimental data and those of Lee and Maddin, Girifalco and Grimes, etc.

Eqn. (43) when used in conjunction with the data presented in Figs. (13. 14) gives the following values for ΔH_p,

Nickel (this investigation) $\Delta H_p = 28,000$ Cal/nole
$= 0.42\ \Delta H_{sd}$

Silver (Lee and Maddin)[8] $\Delta H_p = 20,000$ Cal/nole
$= 0.405\ \Delta H_{sd}$

Where

ΔH_{sd} = the activation energy for self diffusion

These values are in excellent agreement (within the experimental error of our experiment) with those obtained by other investigators by different techniques, e. g.,

Ag (Hoffman and Turnbull)[15] $\Delta H_p = 0.408 \Delta H_{s.d.}$

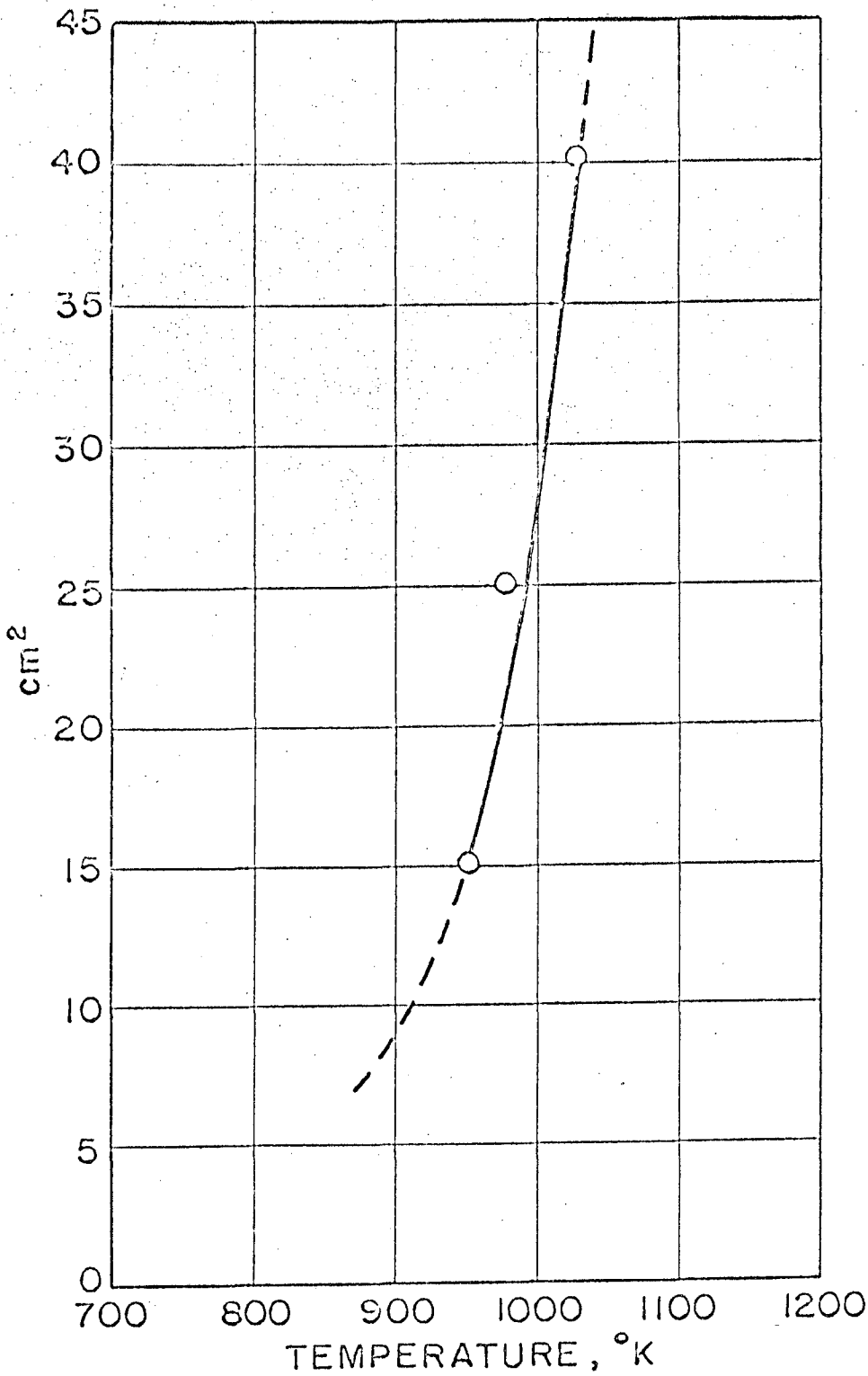

FIG. 16 A PLOT OF $\left(\frac{\bar{D}_s - D_u}{\dot{\varepsilon}}\right) \times 10^{10}$ vs. TEMPERATURE, °K.

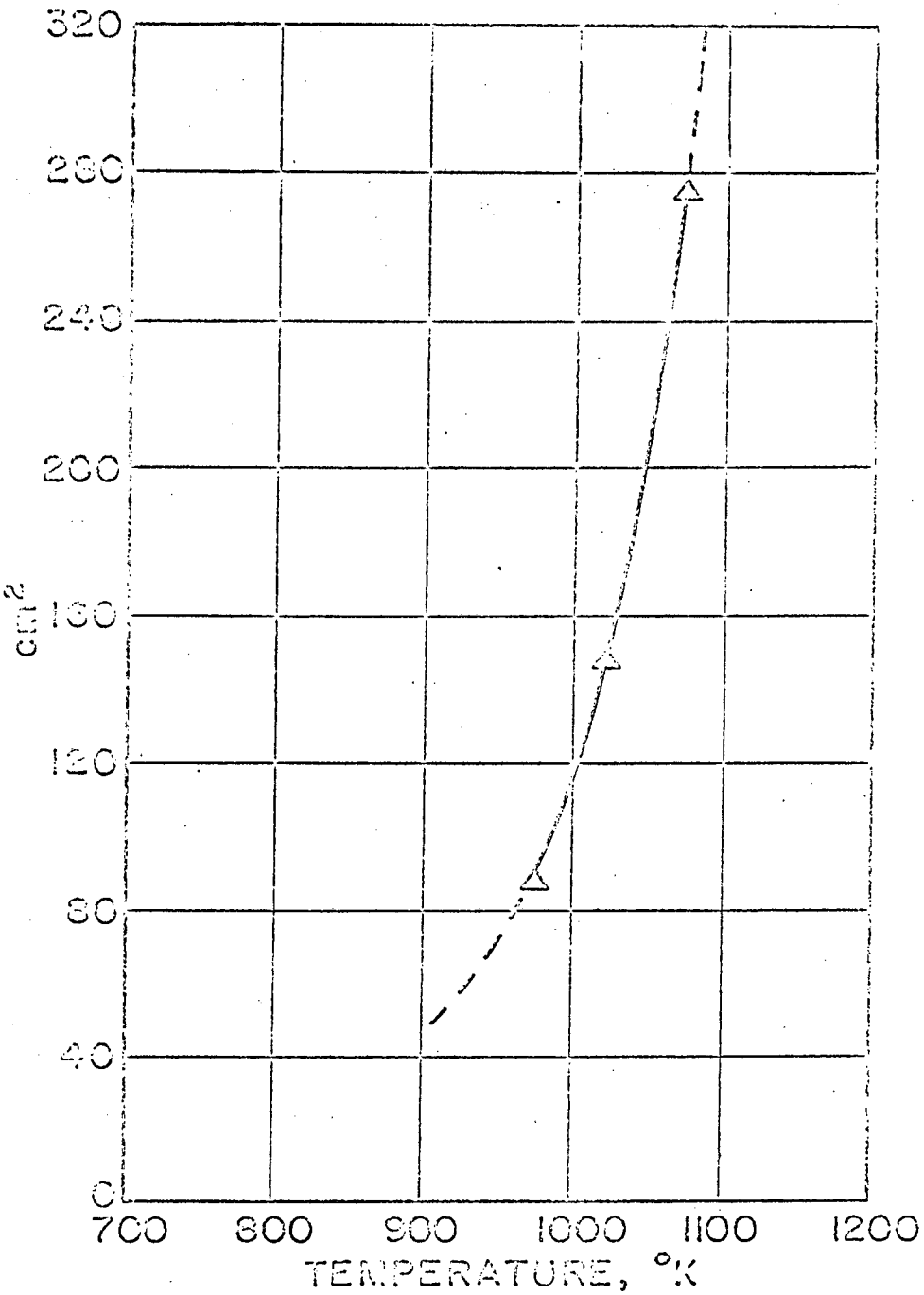

FIG. 17 A PLOT OF $\left(\frac{\bar{D}_s - D_u}{\varepsilon}\right) \times 10^{10}$ vs. TEMPERATURE, °K.

Fe (Bokstein et al) $\Delta H_p = 0.470\ \Delta H_{sd}$

The transient nature of the curves shown in Figs. (12, 12a) is in harmony with the fact that upon the onset of deformation substructure is formed and the density and velocity of moving dislocations changes continuously until the equilibrium substructure is reached whereupon the dislocation density becomes constant and the diffusion coefficient reaches its steady state value. It is to be noted that the steady state substructure and hence the steady state number of moving dislocations and their velocities is a function of temperature and stress and hence a function of strain rate.[29]

Remarks

The model for short circuiting along moving dislocations described in this section which lead to Eqn. (43), explains satisfactorily the dependence of the observed diffusion coefficient in our experiments on temperature and strain rate.

For the enhancement obtained in our experiments this model requires that the vacancies concentration in the immediate neighborhood of the dislocations n, be less or equal one and a half times the equilibrium concentration n_o.

SUMMARY AND CONCLUSIONS

It has been found that the coefficient of self-diffusion in nickel single crystals subjected to tensile straining increases with time up to an asymptotic steady state value which is proportional to the strain rate at a constant temperature. At the lower temperature the diffusion coefficient increases greatly with strain rate.

It has also been found that the coefficient of self-diffusion in prestrained single and polycrystals was independent of the degree of prestrain, and equal to that of the annealed single and polycrystals correspondingly.

It has been found that the coefficients of self-diffusion in fine-grained ($d \leq 0.1$ m m) nickel crystals over the temperature range 675 C to 750 C was a factor 2 to 4 larger than the corresponding coefficients for single crystals.

ACKNOWLEDGEMENT

The author wishes to express his deep appreciation to the Office of Scientific Research and the Atomic Energy Commission for their support of this investigation. He also thanks the International Nickel Company for their gift of the high purity nickel used in this investigation. The author particularly wishes to express his appreciation to Mr. R. Benson for his assistance in developing some of the experimental techniques, and to Mr. S. Rajnak, J. Mote and Dr. J. Simmons for helpful comments concerning experimental procedures and analysis of the data. Special thanks are extended to Mr. D. Singmaster for his invaluable assistance in preparing the specimens and executing the experiments. He also thanks Mrs. V. Tuncer and Miss Kathy Buck for typing the manuscript.

APPENDIX I

Electropolishing and Electroplating Techniques

Electropolishing methods described in the literature gave poor results. It was necessary to develop a new method for electropolishing the specimens. The following method, developed by R. Benson, gave satisfactory results:

Electropolishing solution:

580 cc H_2SO_4 (density 1.84)

435 cc H_2O

5 gm P-toluenesulfonic acid

Current density: 0.4 amp/cm^2

Time: 4-5 minutes

After each specimen was polished, the radioactive nickel isotope was deposited on its surface from a 1% radioactive nickel solution. It was found necessary to activate the surface prior to plating in order to avoid "peel off" of the deposited layer. Deactivation of the surface may have been due either to the formation of a thin oxide layer on the surface, or to a change in the energy levels of the transition electrons (d orbitals). The following method was used for plating:[5]

1) The specimen was electropolished.

2) It was rinsed with running water.

3) The specimen was made the cathode in a basic solution to activate the surface (H_2 is evolved):

Solution:

85 g NaOH/gal.

54 g Na_2CO_3/gal.

Current density: 3 amps/cm^2

Time: 2-3 minutes.

4) Rinsed with running water for two minutes.

5) Plated.

Solution:

115 g $NiCl_2 . 6H_2O$ g/liter

22 g NH_4OH/liter

Current density: .05 amp/m^2

Time: 2 minutes

APPENDIX II

When the creep rate and the generation of vacancies is controlled by both the glide of jogged screw dislocations and the climb of edge dislocations, and when both mechanisms are operating simultaneously, one may write for the creep rate:

$$\dot{E}_{net} = \dot{E}_j + \dot{E}_c \tag{1}$$

where $\dot{E}_{net}$ = total creep rate,

$\dot{E}_j$ = the creep rate due to the motion of vacancy producing jogs,

$\dot{E}_c$ = the creep rate due to the climb of edge dislocations.

The rate of formation of vacancies during the glide of jogged screw dislocations:

The creep rate $\dot{E}_j$ is given by

$$E = (\rho_s \, l_j \, b^2 \nu_j / l_j) \tag{2}$$

where ρ_s = density of screw dislocations,

l_j = the distance between jogs,

ρ_s / l_j = number of jogs per unit volume,

b = the Burgers vector

$l_j \, b$ = area swept out per activation of a jog,

ν_j = the frequency of a thermal activation, " the net frequency for the forward motion of a jog".

If the jogs are superjogs having an average length of P_s atoms the rate of production of excess vacancies per unit volume $\dot{n}_j^+$ is given by

$$\dot{n}_j^+ = \rho_s \, P_s \, \nu_j / l_j \tag{3}$$

Combining Eqn. (2) and (3) one obtains for the rate of production of vacancies:

$$\dot{n}_j^+ = p_s \dot{E}_j / l_j \; b^2 \qquad (4)$$

where $\dot{n}_j^+$ = the rate of production of vacancies per unit volume by jogged screw dislocations,

P_s = the average height of a jog on a screw dislocation.

Next we shall derive an expression for the rate of production of vacancies during the climb of edge dislocations. Let us consider the dislocations configuration shown in Fig.17, where two dislocations sources spaced a distance, 2 L_1, apart operate on two parallel planes a distance 2 h apart. The two sources will continue to operate until such time when the back stress at each source becomes equal to the stress acting on the source. The dislocations in the, i^{th}, array will exert a stress on the dislocations in the, j^{th}, array and vice versa. For a given stress the equilibrium configuration shown in Fig. 1 will be attained. However, if the i and j dislocations were each to climb a height h in time t and annihilate each other then the equilibrium will be upset and the sources will emit a dislocation per each climbing dislocation, and each dislocation in the two arrays will move forward to the next position. If the dislocations are of length, L_2, then the total area swept out per event of climb is

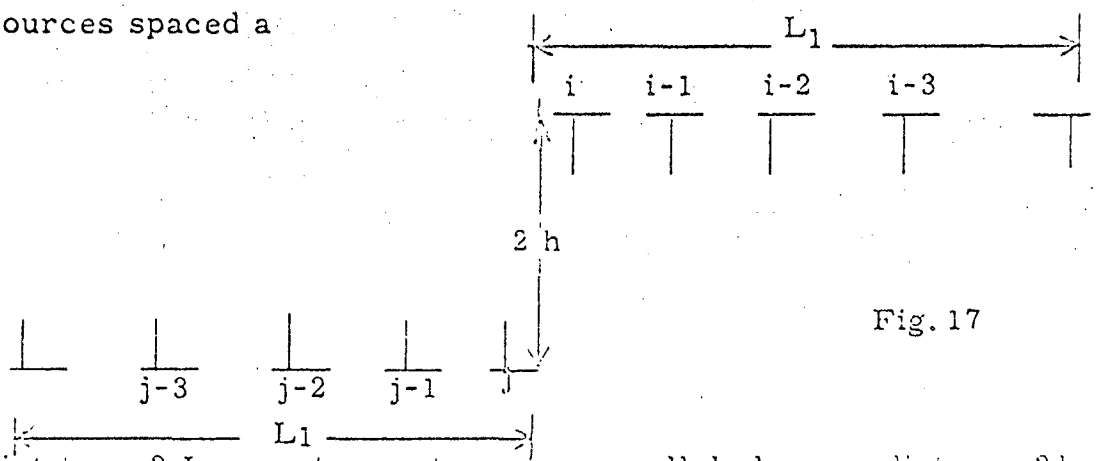

Fig. 17

equal to $(2L_1\ L_2)$. And if the number of such arrays per unit volume is equal to pF where p is the density of edge dislocations and F a constant less than unity, then the strain rate due to the climb of edge dislocations will be given by

$$\dot{E}_c = 2\ L_1 L_2 b\ p\ F / t \tag{5}$$

or

$\dot{E}_c$ = frequency with which the leading dislocation climb x the volume swept out per activation, $2\ L_1 L_2 b\ p\ F$

Hence

$$\dot{E}_c = \nu_c 2\ L_1 L_2 b\ p\ F \tag{6}$$

Now the number of vacancies emitted per single event of climb per unit volume is equal to $(L_2 / b)\ (2h/b)(p\ F)$

and the rate of production of vacancies during climb $\dot{n}_c$ per unit volume is equal to

$$\dot{n}_c^+ = \nu_c (L_2 / b)\ (2h / b)\ (p\ F) \tag{7}$$

Combining Eqns. (6 and 7) one obtains for $\dot{n}_c^+$

$$\dot{n}_c^+ = (h / L_1 b^3)\ \dot{E}_c \tag{8}$$

Now we can combine the terms $\dot{n}_j^+$ and $\dot{n}_c^+$ Eqns. (4 and 8) to obtain the total rate of production of vacancies $\dot{n}^+$ per unit volume.

$$\dot{n}^+ = \dot{n}_c^+ + \dot{n}_j^+ = (p_s\ \dot{E}_j / l_j\ b^2) + (h \dot{E}_c / L_1 b^3) \tag{9}$$

Excess vacancies migrate to sinks which are probably also dislocations. If the dislocations sinks are a distance, L, from the sources, then the mean life time T of an excess vacancy is approximately equal to

$$T = L^2 / 4 D_v \tag{10}$$

where D_v = the diffusivity of a vacancy

Let the rate of disappearance of excess vacancies per unit volume be proportional to their concentration, then

$$\dot{n}^- = (n - n_o)\, 4\, D_v / L^2 \tag{11}$$

where n_o = the equilibrium number of vacancies.

Combining Eqns. (9) and (11) one obtains for the net rate of production of vacancies $\dot{n}$,

$$\dot{n} = (p_s \dot{E}_j / l_j b^2) + (h\, \dot{E}_c / L_1 b^3) - (4\, D_v (n - n_o)/L^2) \tag{12}$$

integrating Eqn. (12) and observing that $n=n_o$ at $t=0$ one obtains

$$n = n_o + \frac{L^2}{4\, D_v}\left[\left(\frac{h}{L_1 b^3}\dot{E}_c + \frac{p}{l_j b^2}\dot{E}_j\right)\left(1 - e^{-4D_v t/L^2}\right)\right] \tag{13}$$

Since the self-diffusivity, D, is equal to

$$D = n \Omega D_v \tag{14}$$

where n = the number of vacancies and

Ω = the atomic volume

therefore

$$D = D_u + \frac{L^2 \Omega}{4}\left(\frac{h}{L_1 b^3}\dot{E}_c + \frac{p_s}{l_j b^3}\dot{E}_j\right)\left(1 - e^{-4D_v t/L^2}\right) \tag{15}$$

where

$$D_u = n_o \Omega D_v$$

In order to obtain a direct comparison with the experimental data given in Fig. 12a, we note that

$$\frac{\int_o^{\dot{\epsilon}} D\, dt}{t} = D_u + \frac{\dot{E}\, L^2 \Omega}{4}\left[\left(\frac{h}{L_1 b^3}\frac{\dot{E}_c}{\dot{E}} + \frac{p_s}{l_j b^2}\frac{\dot{E}_j}{\dot{E}}\right)\left(1 + \frac{L^2}{4 D_v t}\, e^{-4D_v t/L^2}\right)\right] \tag{16}$$

or

$$1/\dot{E}\left(\int_0^t D\,dt/t - D_u\right) = \sqrt{\pi}L^2/4\left\{(h/L_1b^3)(\dot{E}_c/\dot{E}) + (p_s/l_jb^2)(\dot{E}_j/\dot{E})\right\}\left\{1 + \frac{L^2}{4D_vt}e^{-4D_vt/L^2}\right\} \quad (17)$$

Replotting the data in terms of $1/\dot{E}\left(\int_0^t D\,dt/t - D_u\right)$ as a function of t as shown in Fig. 12a reveals that the diffusivity increases with straining and finally reaches a steady state value that is determined by the temperature. For steady state conditions

$$D\,dt = \bar{D}_s\,t$$

and Eqn. (17) reduces to

$$1/\dot{E}\,(\bar{D}_s - D_u) = \sqrt{\pi}L^2/4\left\{(h/L_1b^3)(\dot{E}_c/\dot{E}) + (p_s/l_jb^2)(\dot{E}_j/\dot{E})\right\} \quad (18)$$

or

$$\bar{D}_s - D_u = \sqrt{\pi}L^2/4\left\{(h/L_1b^3)(\dot{E}_c/\dot{E}) + (p_s/l_jb^2)(\dot{E}_j/\dot{E})\right\}\dot{E} \quad (18a)$$

A plot of $(\bar{D}_s - D_u)$ as a function of strain rate, $\dot{E}$, is presented in Fig. 13, where it appears that the slope is an increasing function of temperature. The slope $(1/\dot{E})(\bar{D}_s - D_u)$ is given by

$$\text{Slope} = \sqrt{\pi}L^2/4\left\{(h/L_1b^3)(\dot{E}_c/\dot{E}) + (p_s/l_j\,b^2)(\dot{E}_j/\dot{E})\right\} \quad (19)$$

and is plotted in Fig. 16 as a function of temperature.

Since the present data (Fig 16) does not allow one to establish the exact dependence of the term given by Eqn. (19) on temperature we shall resort to a theoretical analysis of this term.

Of the various quantities that appear in the expression for the slope (Eqn. (19) only the following may be temperature dependent:

P_s:

P_s is the average height of a jog on a screw dislocation. If the jogs are formed mechanically for example during intersection, etc., Ps will be independent of temperature. However, if the jogs are thermal jogs P_s will depend on the temperature. But since the energy to form a jog increases with the height of the jog wewe shall take Ps to be equal to unity from energy consideration.

l_j:

l_j is the average distance between jogs; again, if the jogs are mechanical jogs, l_j will be independent of temperature, however, if the jogs are thermal, one may write for l_j

$$l_j = b\, e^{g_j/k\,T} \tag{21}$$

where

g_j = the free energy to form a jog.

$\dot{E}_j$:

$\dot{E}_j$ is the creep rate arising from the glide of jogged screw dislocations. According to J. E. Dorn[25] $\dot{E}_j$ has the following form

$$\dot{E}_j = P_s b^2 \nu\, e^{-g_{s.d}/l_a T}\left\{ e^{\frac{\tau l_j b^2/P_s}{l_a T}} - e^{-\frac{\tau l_j b^2/P_s}{l_a T}} \right\} \tag{22}$$

or

$$\dot{E}_j = 2 P_s b^2 \nu \sinh\left(\frac{\tau l_j b^2/P_s}{l_a T}\right) e^{-g_{s.d}/l_a T} \tag{22a}$$

where T = the applied stress,

$g_{d.s.}$ = the activation energy for self-diffusion,

= the Debye frequency,

Ps, P_s, b same as above.

$\dot{E}_c$ is the creep rate arising from the climb of edge dislocations and may be written as follows:[25]

$$\dot{E}_c = 16\pi^2(1-\mu)^2 \nu \Xi N \left(\frac{\tau}{G}\right)^2 e^{-\left(\frac{\theta_{s.d} + \theta_j''}{\lambda_2 T}\right)} \times \left\{ e^{\frac{8\sqrt{2}\pi^2(1-\mu)^2 \delta^2 \tau^3 \nu}{G^2 b^2 \lambda_2 T}} - e^{\frac{8\sqrt{2}\pi^2(1-\mu)^2 \delta^2 \tau^3 \nu}{G^2 b^2 \lambda_2 T}} \right\} \quad (23)$$

or

$$\dot{E}_c = 32\pi^2(1-\mu)^2 \nu \Xi N \left(\frac{\tau}{G}\right)^2 \sinh\left(\frac{8\sqrt{2}\pi^2(1-\mu)^2 \delta^2 \tau^3 \nu}{G^2 b^2 \lambda_2 T}\right) \times e^{-\left(\frac{\theta_{s.d} + \theta_j''}{\lambda_2 T}\right)} \quad (23a)$$

for stresses up to the order of 10^9 dynes/cm^2 the argument of the sink term is small compared to unity and the sink can be replaced by its argument. Thus, the expression for $\dot{E}_c$ becomes

$$\dot{E}_c = \frac{256(1-\mu)^4 \pi^4 \nu \Xi N \nu \delta^2 \tau^5}{G^4 b^4 \lambda_2 T} e^{-\left(\frac{\theta_{s.d} + \theta_j''}{\lambda_2 T}\right)} \quad (24)$$

Substituting Eqns. (22a) and (24) into Eqn. (18a) one obtains:

$$D_s - D_d = \frac{\nu L^2}{4} \left\{ \frac{\lambda_1}{L_1 b^3} \frac{1}{1 + \frac{P_s b^6 G^4 \lambda_2 T \sinh(\tau^2 \lambda_1 b^2 / P_s \lambda_2 T)}{180(1-\mu)^4 \pi^4 \Xi N \nu \delta^2 \tau^5} e^{\theta_j'/\lambda_2 T}} + \right.$$
$$\left. + \frac{P_s}{\lambda_1 b^2} \frac{1}{1 + \frac{180(1-\mu)^4 \pi^4 \Xi \nu \delta^2 \tau^5}{P_s b^6 G^4 \lambda_2 T \sinh(\tau^2 \lambda_1 b^2 / P_s \lambda_2 T)} e^{-\theta_j'/\lambda_2 T}} \right\} \dot{E} \quad (25)$$

For stresses in the range of 10^6 to 10^9 dynes/cm^2 the second term in the bracket in Eqns. (25) is small compared to the first term and Eqn. (25) reduces to:

$$D_s - D_d = \dot{E} \left\{ \frac{45\nu^2 L^2 \lambda_1 (1-\mu)^4 \pi^4 \Xi \nu \delta^2 \tau^5}{L_1 P_s b^9 G^4 \lambda_2 T \sinh\left(\frac{\tau^2 \lambda_1 b^2 / P_s}{\lambda_2 T}\right)} e^{-\theta_j'/\lambda_2 T} \right\} \quad (26)$$

Eqn. (26) shows the variation of $D_s - D_u$ with strain rate and temperature which is in qualitative agreement with the experimental data presented in Figs. 12a and 12b.

APPENDIX III

Hendrickson and Machlin[26] gave the following estimate for the effective diameter, d, of a dislocation,

$$d = 10^{-7} \text{ cm}$$

For a dislocation density, p, the fraction of atoms, f, that are in dislocations per unit volume is given by

$$f = d^2 p \; / \; 4a^3 n_s$$

where

a = the interatomic distance

n_s = the number of sites per unit volume (using the above value for d one obtains the following value for f in nickel)

$$f = 5 \times 10^{-15} p$$

f as a function of the dislocation density, p,

Cm/Cm^3 p	10^6	10^7	10^8	10^9	10^{10}	10^{11}
f	$5x10^{-9}$	$5x10^{-8}$	$5x10^{-7}$	$5x10^{-6}$	$5x10^{-5}$	$5x10^{-4}$

REFERENCES

1. S. Chandrasekhar, Rev. Mod. Phys. 15, 1 (1943).

2. F. S. Buffington and M. Cohen, J. of Met. 4, 859 (1952).

3. N. Ujiiye, B. L. Averbach, and M. Cohen, Acta Met. 6, 68 (1958).

4. H. H. Grimes, Acta. Met. 7, 782 (1959).

5. A. F. Forestieri and L.

6. J. B. Darby, C. T. Tomizuka and R. W. Baluffi, J. Appl. Phys. 30, 104 (1959).

7. A. F. Brown, Radioisotope Conference, Copenhagen, Met. and Solid State Physics (1960).

8. C. H. Lee and R. Maddin, Trans. AIME, 215, 397 (1959).

9. A. V. Savitskii, Report to the Conference on Defects in Crystal Structure and the Properties of Metals and Alloys (Kiev, 1959).

10. L. M. Shestopalov and Yu. P. Romashkin, (a) Report to the All Soviet Conference on Strength Physics (Karkov, 1958); (b) Fiz. Tverd. Tela, 2, 2998 (1960).

11. S. Z. Bokstein, et. al., (a) Certain problems connected with the Strength of Solids, (KZd ANNSSSR, 1959) P. 76; (b) Report to the Conference on Defects in Crystal Structure and the Properties of Metals and Alloys (Kiev, 1959).

12. V. S. Mikhalenkov, Dissertation (Kiev, 1958).

13. Dorn, J. E. and Simmons, J., Appl. Phys., Vol. 29, No. 9, 1308, Sept., 1958.

14. Benson, R., Master's Thesis, University of California, 8, 1960.

15. R. E. Hoffman and D. Turnbull. J. Appl. Phys. 22, 634 (1951).

16. Hoffman, R. E., Pikus, F. W., and Ward, R. A., AIME, J. of Metals, 8, 483 (1956).

17. Reynolds, J. E., Averbach, B. L., and Cohen, M., Acta Met. 5, 29, (1957).

18. Messner, A., Benson, R., and Dorn, J. E., ASM, No. 193, 1960.

19. Hirano, Cohen, and Averbach, private communication.

20. D. Turnbull, Am. Soc. Metals Seminar on "Atom Movements". Chicago, 1950.

21. J. C. Fisher, J. Appl. Phys. 22, 74 (1951).

22. J. W. Henderson and J. S. Kochler, Phys. Rev. 104, 626, (1956).

23. J. E. Dorn, Gillet Memorial Lecture, ASTM, (1962).

24. A. A. Hendrickson and E. S. Machlin, Trans., AIME 1035, (1954).

25. R. E. Hoffman and D. Turnbull, Acta Met. 2, 419 (1954).

26. E. W. Hart, Acta Met. 5, 597 (1957).

27. Raymond and Dorn on creep and recovery, private communication.

28. A. L. Ruoff and R. W. Balluffi, Cornell University, Mat. Sci. Center, Report No. 46, (1962).

29. A. L. Ruoff and R. W. Balluffi, Cornell University, Mat. Sci. Center, Report No. 48, (1962).